Applied Energy 283 (2021) 116277

Contents lists available at ScienceDirect

Applied Energy

journal homepage: www.elsevier.com/locate/apenergy

Applications and technological challenges for heat recovery, storage and utilisation with latent thermal energy storage

Zhi Li [a,b], Yiji Lu [a,c,*], Rui Huang [a], Jinwei Chang [a], Xiaonan Yu [a], Ruicheng Jiang [a], Xiaoli Yu [a,b,*], Anthony Paul Roskilly [a,c,*]

[a] Department of Energy Engineering, Zhejiang University, Hangzhou 310027, China
[b] Ningbo Institute, Zhejiang University, Ningbo 315100, China
[c] Durham Energy Institute, Durham University, Durham DH1 3LE, United Kingdom

HIGHLIGHTS

- Enhancement methods of thermal conductivity for medium-high temperature PCMs.
- Design and optimisation strategies for LTES heat exchangers.
- LTES energy systems for heat recovery, storage and utilisation.
- An in-depth summary of the medium-high temperature LTES materials.

ARTICLE INFO

Keywords:
Latent thermal energy storage
Phase change materials
Thermal conductivity enhancement
Heat transfer enhancement
Heat recovery

ABSTRACT

Thermal energy storage (TES) technology is considered to have the greatest potential to balance the demand and supply overcoming the intermittency and fluctuation nature of real-world heat sources, making a more flexible, highly efficient and reliable thermal energy system. This article provides a comprehensive state-of-the-art review of latent thermal energy storage (LTES) technology with a particular focus on medium-high temperature phase change materials for heat recovery, storage and utilisation. This review aims to identify potential methods to design and optimise LTES heat exchangers for heat recovery and storage, bridging the knowledge gap between the present studies and future technological developments. The key focuses of current work can be described as follows: (1) Insight into moderate-high temperature phase change materials and thermal conductivity enhancement methods. (2) Various configurations of latent thermal energy storage heat exchangers and relevant heat transfer enhancement techniques (3) Applications of latent thermal energy storage heat exchangers with different thermal sources, including solar energy, industrial waste heat and engine waste heat, are discussed in detail.

1. Introduction

Tackling climate change, providing energy security and delivering sustainable energy solutions are major challenges faced by civil society. Improved thermal energy conversion and utilisation results in reduced emissions, more sustainable economy for industrial and domestic consumers and supports a more stable energy security position [1]. One of the key research challenges in real-world thermal energy systems is how to overcome the thermal power fluctuations enabling efficiently and effectively use the heat sources such as solar, industrial waste heat and geothermal energy [2,3].

1.1. Thermal energy storage technologies

Thermal Energy Storage (TES) is a crucial and widely recognised technology designed to capture renewables and recover industrial waste heat helping to balance energy demand and supply on a daily, weekly or even seasonal basis in thermal energy systems [4]. Adopting TES technology not only can store the excess heat alleviating or even eliminating the thermal power fluctuations but also mitigate the mismatching in

* Corresponding authors at: Department of Energy Engineering, Zhejiang University, Hangzhou 310027, China.
E-mail addresses: luyiji0620@gmail.com (Y. Lu), yuxl@zju.edu.cn (X. Yu), anthony.p.roskilly@durham.ac.uk (A.P. Roskilly).

https://doi.org/10.1016/j.apenergy.2020.116277
Received 17 June 2020; Received in revised form 12 November 2020; Accepted 13 November 2020
Available online 9 December 2020

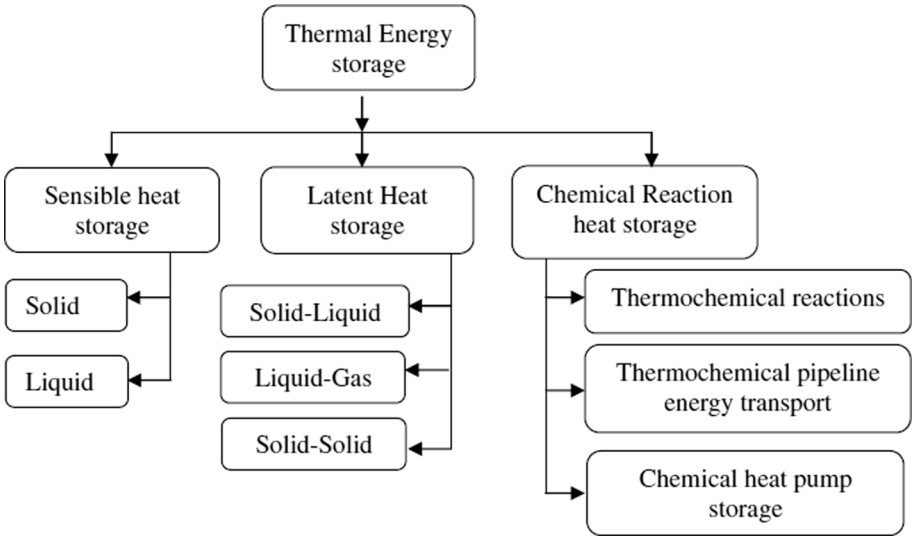

Fig. 1. Classification of thermal energy storage technologies [6].

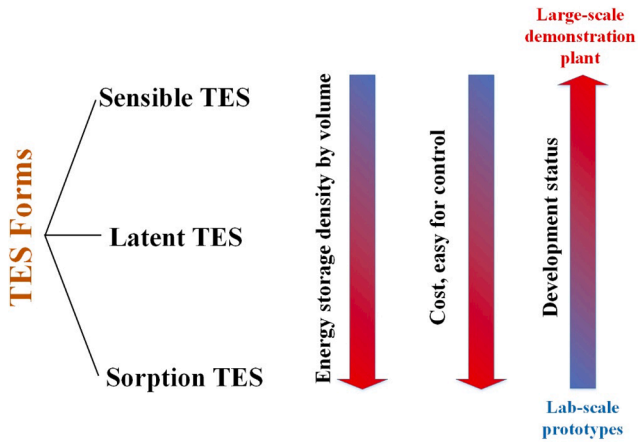

Fig. 2. Characteristics of different TES systems [7].

time and location between the energy supply and corresponding demand from consumers [5]. TES technologies can be classified into three categories including Sensible Thermal Energy Storage (STES), Latent Thermal Energy Storage (LTES) and Thermo-Chemical (Sorption) Energy Storage (TCS) as shown in Fig. 1.

Each thermal energy storage technology has its advantages and disadvantages as shown in Fig. 2. LTES has the advantages of comprehensive large energy storage density, compact in size and high technical feasibility to be used for renewable energy storage, waste heat recovery (WHR) and thermal power buffering in industrial processes.

1.2. The original and unique contribution of this work

The integration and utilisation of latent thermal energy storage (LTES) with heat recovery systems is the most potential, cost-effective solution and has been widely investigated worldwide. Previously reported reviews on the similar research topic are reviewed and summarised as follows. Kenisarin [8] conducted a review of different kinds of high-temperature PCMs for LTES devices. Gil et al. [9,10] summarised high-temperature thermal energy storage considering the concepts, materials, models and applications for solar power generation. Bruno et al. [11] reviewed high-temperature PCMs, performance improvement techniques and design considerations for solar power generation systems. Xu et al. [12] reported on recent technical developments of LTES for different applications, particularly concentrated solar power generating systems. Laia et al. [13] presented a review about applications of PCM-based TES on the industrial waste heat recovery including the manufacturing process, vehicle engines and power plants. Li et al. [7] reviewed the different energy systems integrated into a TES unit with a particular focus on LTES and their performance from the perspective of sustainable energy utilization. Ibrahim et al. [14] reviewed several different heat transfer enhancement methods, considering the geometric design and thermal conductivity improvement for LTES storage systems. Tao et al. [4] focused on phase change materials and enhancement of thermal conductivity, as well as heat transfer enhancement techniques for LTES systems in the past decade. Focusing on the molten salt PCMs, Li et al. [15] reviewed the performance investigation and enhancement techniques for medium and high-temperature applications. Analysing the existing reviews related to LTES technology, we find there is no review providing a comprehensive summary focusing on the medium-high temperature PCMs and their applications in various thermal energy systems.

The LTES using medium-high temperature PCMs shows different characteristics, which has different requirements in component-level design and system-level application, compared to the commonly used low-medium temperature PCMs. For example, the salts and metals (medium-high temperature PCMs) possess different thermophysical properties from the paraffin (low-temperature PCM). Currently, there are a very limited number of reviews focusing on the LTES heat exchangers especially those using medium-high temperature PCMs comparing the compare the difference in heat transfer enhancement techniques for different types of LTES such as shell-and-tube LTES and cylindrical LTES. The integration of LTES with heat recovery technology has a great potential to overcome the intermittence and fluctuation of real-world thermal sources balancing the energy supply and demand. Although there are some related reviews on LTES published in the last five years, it is timely important and urgent need to provide new insights using medium-high temperature PCMs in heat recovery, storage and utilisation.

As the above-mentioned reasons, we develop this review article focusing on the applications and challenges of LTES with medium-high temperature PCMS in terms of modelling, simulation and experiments of material-level (LTES materials - Phase Change Materials), component-level (LTES heat exchangers) and system-level (integrated LTES with heat recovery systems), as an important reference contributing to and promoting the research progress in thermal energy systems.

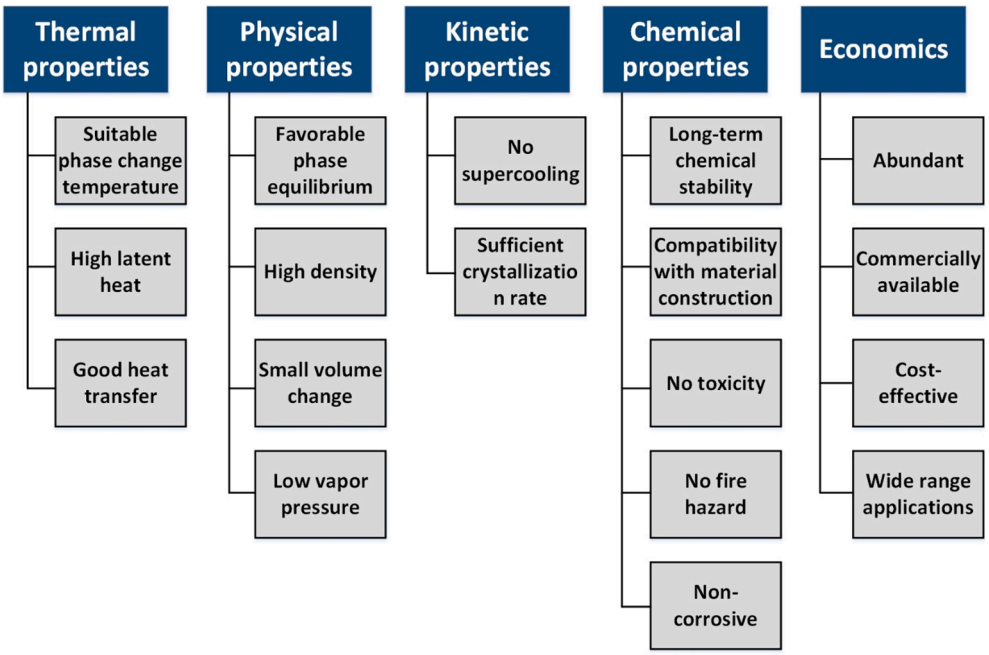

Fig. 3. Requirements for phase change materials [18,19].

1.3. Aim and objectives

This review aims to present the state-of-the-art research comprehensively covering the material level, component-level and system-level of the heat recovery, storage and application of LTES technologies, with a particular interest focusing on the utilisation of medium-high temperature PCMs in thermal energy systems. Specifically, the objectives are

- Material-level overview: Provide an in-depth, critical and comprehensive summary of the thermophysical properties and potential enhancement methods of medium-high temperature PCMs
- Component-level discussion: Conduct a detailed discussion on the design and performance optimisation strategies on the different types of heat exchangers for LTES systems with the potential of providing high energy storage density, improved heat transfer performance and increased thermo-mechanical property
- System-level approach: The application and integration methods of using LTES with heat recovery technologies to achieve the optimal overall energy efficiency were conducted and summarised

2. Medium-high temperature PCMs

A general definition of medium-high temperature PCMs is the materials with a phase change temperature (PCT) over 100 °C [16,17]. The density and latent heat of PCMs determine the energy storage density during the phase change process. Other than the energy storage density, the candidate PCM also significantly depends on the melting temperature, thermochemical stability, corrosion to the container, as well as the cost [12]. To achieve an improved match with LTES systems and objective applications, PCMs should meet a series of requirements, as shown in Fig. 3.

2.1. Categories of medium-high temperature PCM

A broad number of studies have been reported employing different categories of PCMs for LTES in heat recovery applications [20–24]. PCMs are normally classified into three categories based on their Phase Change Temperature (PCT) and material compositions, which are known as organic, inorganic and eutectic, as depicted in Fig. 4.

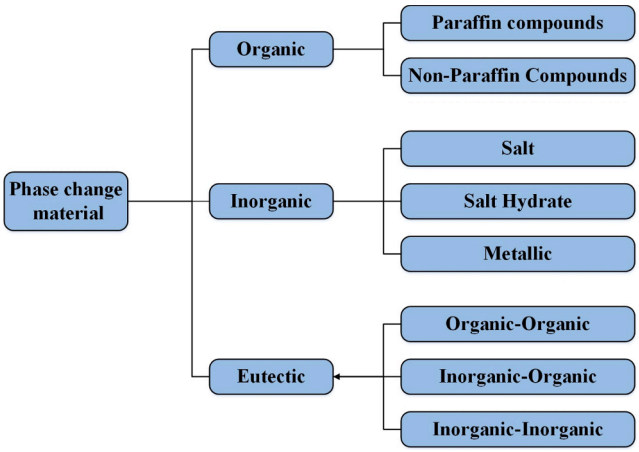

Fig. 4. Classification of PCMs [23,25].

2.1.1. Organic compounds

Organic compound materials have been widely implemented in both domestic and commercial applications, such as buildings, electronic devices, cold storage, solar heating devices, textiles, and waste heat recovery [12]. Organic compound materials are chemically stable, non-toxic, non-corrosive, without phase segregation and are available from nature [26]. However, organic materials suffer from low thermal conductivity ranging between 0.1 and 0.35 W/m K. A small number of organic materials have been explored for heat recovery applications of solar power plants, transport sectors and industries since most organic materials have a relatively low melting temperature. Some organic materials with phase change temperature over 100 °C are listed in Table 1.

2.1.2. Salts and salt compositions

Medium-high temperature salts and salt compositions refer to nitrates, chlorides, carbonates, fluoride, sulfates, as well as their compositions [31,35]. These inorganic materials are generally high in working

Table 1
Thermophysical properties of potential organic compounds PCM with melting temperature over 100 °C [17,20,27–30].

Organic compound	T_m	ΔH	Cp_s	Cp_l	λ_s	λ_l	ρ_s	$E_{density}$	Price	
	°C	kJ/kg	kJ/kg K		W/m K		kg/m^3	kWh/m^3	£/m^3	£/kWh
RT100	100	124	1.80	2.40	0.2	0.2	1630			
Dimethyl fumarate	102	242					1045.2	70.3		
Oxalic acid	105	356	1.62	2.73			1900	211	524	3.9
Hectane	115	285					846	67		
Erythritol	117	340	2.25	2.61	0.73	0.33	1450	148	1287	13.6
HDPE	130	255	2.60	2.15	0.48	0.44	952	80	463	9.0
Phthalic anhydride	131	160	1.85	2.20			1530	85	2042	37.4
Urea	134	250	1.80	2.11	0.80	0.60	1320	97	189	3.0
Glucose	141	174					1544	75		
Maleic acid	141	385	1.17	2.08			1590	184	1059	9.0
2-Chlorobenzoic acid	142	164	1.30	1.60			1544	83	1861	35.1
Xylose-D	147–151	216–280					1530	92–119		
Xylose-L	147–151	213					1530	91		
Adipic acid	152	275	1.87	2.72			1360	109	584	8.4
d-Mannitol	165	300	1.31	2.36	0.19	0.11	1490	139	1027	11.5
Hydroquinone	172	258	1.59	1.64			1300	105	3415	50.9
Galactitol	188–189	351.8					1471	143.6		

Table 2
Thermophysical properties of potential inorganic salts PCM with melting temperature more than 100 °C [11,12,27,31–33].

Inorganic salts	Melting temperature (°C)	Latent heat (kJ/kg)	Density (kg/m^3)	Energy density (kJ/m^3)	Thermal conductivity (W/m K)
$ZnCl_2$	280	75	2907	218.025	0.5
$NaNO_2$	282	212			
$NaNO_3$	308	199	2257	449.143	0.5
NaOH	318	165	2130	346.500	0.92
KNO_3	336	116	2110	244.760	0.5
KOH	380	149.7	2044	305.987	0.5
AgBr	432	48.8	6473		
LiI	458	109	3490		
LiOH	462	873	1460		
$PbCl_2$	501	78.7	5600		
SrI_2	527	57	4550		
LiBr	550	203	3460		
$Ba(NO_3)_2$	594	209	3230		
LiCl	610	441	2070		
MgI_2	633	93	4430		
NaI	661	158	3670		
$MgCl_2$	714	452	2140	967.280	
NaCl	800	492	2160	1062.720	5.0
Na_2CO_3	854	275.7	2533	698.348	2.0
K_2CO_3	897	235.8	2290	539.982	2.0
NaF	996	794	2558		

temperature, thermal stability, specific heat and convective heat transfer coefficient at liquid state, while they are low in viscosity, saturated vapour pressure and price. Pure salts have predetermined thermophysical properties, while salt compositions provide additional options to modify the thermophysical properties of pure salts, extending the working temperature range and creating opportunities to use more PCMs to meet the requirements of LTES systems. A large number of pure salts are available to form different combinations of salt compositions, therefore, it is currently a challenge to predict the thermophysical properties for salt compositions because of limited experimental data. Raud et al. [36] conducted a detailed review to conclude the theoretical formulas and geometric methods to predict the thermophysical parameters of salt combinations based on the known salts.

As is shown in Table 2 and Table 3, it can be seen that many salts and salt compositions, with a melting temperature in the range of 150–400 °C, are quite suitable to be used in heat recovery technologies [12,37]. Among all the salts and salt compositions, $NaNO_3$, KNO_3 and their compositions have been extensively used in solar power plants due to their proper melting temperature and relatively high latent heat [38,39]. From the design perspective, low working temperature is desirable to reduce the operational and maintenance costs of the system. Recently, lithium salts have received increasing attention due to their low melting temperature, low density and high latent heat [40]. Lithium salts have been added and mixed with other salts to form salt compositions used in solar power plants. As the results presented in Fig. 5, the benefits of lithium salt additives can reduce the melting temperature, expand the working temperature and improve thermal stability compared with a commercial salt composition ($34KNO_3$-$66NaNO_3$).

2.1.3. Metallic materials

Metallic materials include metals with a low melting temperature and their alloys. The most prominent advantages of metallic materials are the high thermal conductivity and energy storage capacity per volume unit [42]. The large energy storage capacity is attractive for LTES systems with volume limitation while the high thermal conductivity eliminates the requirement of exploring additional techniques for heat conduction enhancement [43]. Metallic materials with abundant thermophysical property data for PCM design is significantly lower in proportion to the substantial number of available metals and alloys. Some metallic materials are summarised and listed in Table 4. Experimental studies on thermal properties of metallic materials are quite limited. Only melting temperature and latent heat are available for most of the metals and alloys [44].

Although Birchena et al. [32,45] conducted early studies to explore the potential application of metals and alloys as PCMs for energy storage, metallic materials have not been extensively considered as PCMs in real-world heat recovery applications. Because these materials possess high density and low specific latent heat per mass unit, they are not suitable for the application under weight-sensitive conditions [46]. More recently, some preliminary studies were conducted to investigate the thermal properties and heat transfer performance of aluminium-based and magnesium-based alloys [47–51], which demonstrated the advantages of the metallic materials with low melting temperature metals over the conventional salts, as well as demonstrating their promising applications in solar power plants, steam generation systems and industrial processes. More detailed properties of metallic materials as PCMs have been summarised in the recent reviews reported by Cabeza et al. [52], Crespo et al. [53] and Zhang et al. [35].

2.2. Thermal conductivity enhancement

Unlike metallic materials, most of the organic materials and inorganic salts have very low thermal conductivity, which leads to adverse effects on the heat transfer and energy storage performance of LTES systems during the charging-discharging process. The most commonly

Table 3
Thermophysical properties of potential inorganic salt composition PCM with melting temperature more than 100 °C [11,12,32–34].

Salt compositions	Mass ratio	Melting temperature °C	Latent heat kJ/kg	Density kg/m^3	Energy density kJ/m^3	Thermal conductivity W/m K
KNO_3-$LiNO_3$-$NaNO_3$-MgK	1:1:1:1	101	158		210	
LiCl-$AlCl_3$	17.5:82.5	114	114	2376		
KNO_3-$LiNO_3$-$NaNO_3$	1:1:1	117	232		423	
KCl-$AlCl_3$	21.6:78.4	128	254	2343		
$LiNO_3$-KNO_3	31.7:68.3	135	135.6	1780		
$LiNO_3$-$NaNO_3$-KCL	55.4: 4.5:40.1	160	266	1905		
$LiNO_3$-KCl	58.1:48.9	166	272	1918		
$LiNO_3$-LiCl-$NaNO_3$	47.9:1.4:50.7	180	267	1986		
$LiNO_3$-$NaNO_3$	57:43	193	248.3	1880		
$LiNO_3$-$NaNO_3$-$Sr(NO_3)_2$	45:47:8	200	199	1993		
$LiNO_3$-NaCl	87:13	208	369	1993		
$LiNO_3$-NaCl	93.6:6.4	220	363	1850		
$NaNO_3$-KNO_3	50:50	220	100.7	1920	193.344	0.56
KCl-$ZnCl_2$	68.1:31.9	235	198	2480	491.040	0.8
$LiNO_3$-Li_2SO_4	98:2	255	354	2357		
LiCl-LiOH	37:63	262	485	1550	751.750	1.1
NaCl-KCl	58:42	360	119	2084.4	248.044	0.48
LiF-LiCl-NaCl-KCl	1.8:39.9:8.3:50	368	523	2048		
LiCl-LiF-Li_2CO_3-LisSO4	29:24:21:26	419	387	2252		
KCl-Li_2SO_4-NaCl	29.6:53.8:16.6	420	586.2	2062		
NaCl-$Sr(NO_3)_2$	26.9:73.1	424	244	2062		
NaBr-$MgBr_2$	45:55	431	212	3490		0.9
KCl-$ZnCl_2$	1:46	432	218	2410		0.83
$MgCl_2$-NaCl	38.5:61.5	435	351	2480	870.480	
$MgCl_2$-NaCl	1:52	450	431	2250		
Li_2CO_3-K_2CO_3	1:53	488	342	2200		1.99
Na_2CO_3-Li_2CO_3	56:44	496	370	2320	858.400	2.09
NaCl/$CaCl_2$	1:67	500	281	2160		1.02
NaF-KF-K_2CO_3	1:21:62	520	274	2380		1.5
NaF-MgF_2	75:25	650	860	2820	2425.200	1.15
LiF-CaF_2	80.5:19.5	767	816	2390	1950.240	3.8

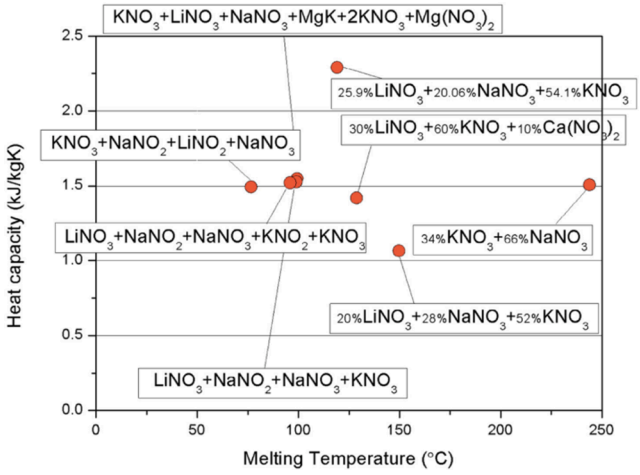

Fig. 5. Heat capacity and melting temperature of some salt compositions with lithium salts [40,41].

used technique for thermal conductivity enhancement is to embed porous media and nanoparticle additives with high thermal conductivity into the PCMs to form PCM compositions [54,55].

2.2.1. Porous media

Porous media should have the characteristic of high thermal conductivity to efficiently enhance the PCM thermal conductivity, as well as high porosity to maintain enough PCM filling ratio and high energy storage density [4]. The commonly used porous media mainly includes metal foam and expanded graphite (graphite foam). Both of them have high thermal conductivity (up to 400 W m^{-1} K^{-1} for metal foam and 300 W m^{-1} K^{-1} for expanded graphite) and high porosity (up to 90%)

Table 4
Thermophysical properties of some metals and alloys with PCM potential [8,31–34].

Metals and alloys	Mass ratio	Melting temperature (°C)	Latent heat (kJ/kg)	Density (kg/m^3)
Zn		419	112	7140
Mg		648	365	1740
Al		661	388	2700
Mg-Zn	46.3:53.7	341	185	4600
Zn-Al	96:4	381	138	6630
Al-Mg-Zn	59:35:6	443	310	2380
Al-Si-Sb	86.4:9.4:4.2	471	471	2700
Mg-Al	34.65:65.35	497	285	2155
Al-Cu-Mg	60.8:33.2:6	506	365	3050
Al-Si-Cu-Mg	64.1:5.2:28:2.2	507	374	4400
Al-Si-Cu	68.5:5:26.5	525	364	2938
Al-Cu-Sb	64.3:34:1.7	545	331	4000
Al-Cu	66.92:33.08	548	372	3600
Al-Si-Mg	83.14:11.7:5.16	555	485	2500
Al-Si	87.76:12.24	557	498	2540
Al-Si-Cu	46.3:4.6:49.1	571	406	5560
Zn-Cu-Mg	49–45-6	703	176	8670
Cu-P	91–9	715	134	5600
Cu-Zn-P	69:17:14	720	368	7000
Cu-Si-Mg	56:27:17	765	125	7170
Mg-Si-Zn	47:38:15	800	314	
Cu-Si	80:20	803	197	6600
Cu-P-Si	83:10:7	840	92	6880
Si-Mg-Ca	49:30:21	865	305	2250
Si-Mg	56:44	946	757	1900

and large specific surface area as shown in Fig. 6. Metal foam is commonly used to enhance the thermal conductivity of organic materials with low melting temperature. While expanded graphite not only can be used as the matrix for low-temperature PCMs but also high-temperature PCMs [57]. As metal foam possesses good chemical

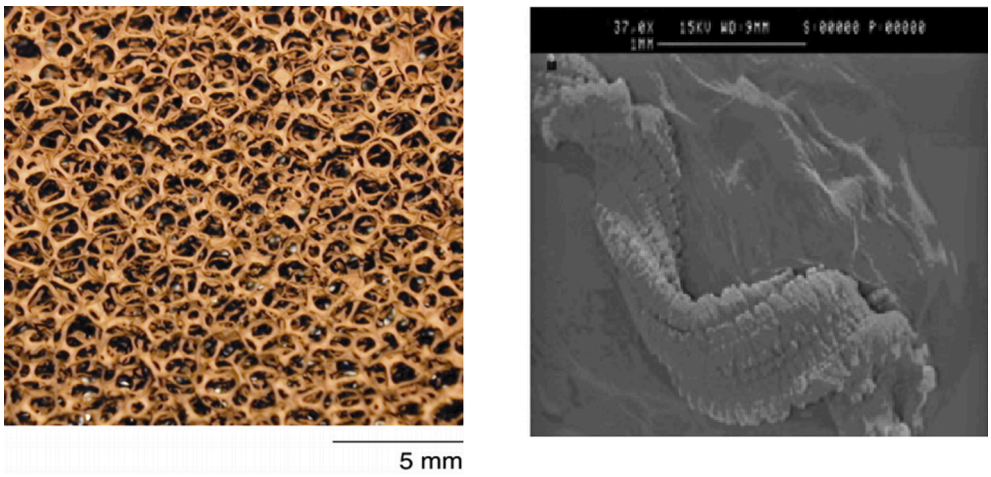

Fig. 6. Structures of porous materials [56]: (a) copper metal foam; (b) expanded graphite.

stability in the low-temperature range and expanded graphite has good chemical stability even in the high-temperature region.

The commonly used metal foams include copper, aluminium and nickel. Aluminium has shown the greatest potential due to its balanced high thermal conductivity and low density. The geometric parameters including porosity and pore size for metal foam show an important influence on the charging-discharging performance of LTES systems, since they determine the percentage of the volume occupied with PCM and hence the energy storage density [40].

It can be concluded from Table 5 that porous materials can potentially improve the thermal conductivity of PCM. However, it is worth noting that both metal foam and expanded graphite reduced the natural convection of liquid PCM during the charging process, and the adverse effect is not observed during the discharging process. For instance, Zhang et al. [58] demonstrated that the natural convection was weakened in the liquid molten-salt with metal foam, while the discharging process was enhanced due to the presence of the metal foam. Zhu et al. [59] obtained similar results that the increase of PPI (pore per inch) of metal foam could suppress the convective heat transfer so that reduce the energy storage performance of the composite PCM. Attention should be paid to the mass/volume fraction in order to balance the trade-off between the thermal conductivity enhancement and natural convection reduction. According to the above discussion and results summarised in Table 5, it can be demonstrated that the melting/solidification process of LTES system can be significantly enhanced with the porous materials. Nevertheless, in this technique, the geometric parameters and mass/volume fraction, which have a significant influence on the performance of LTES systems, should be important considerations. Finally, the elaboration method to prepare composite of PCM and porous material should be a focus of future studies, since PCM composites obtained by different elaboration routes may quite differ in thermal conductivity enhancement.

2.2.2. *Nanoparticle additives*

Carbon nanomaterials are the most commonly used nanoparticle additives as they have high thermal conductivity, stable chemical nature, extensive usability and low density [25]. Carbon nanomaterials mainly include multi-wall carbon nanotube (MWCNT), single-wall carbon nanotube (SWCNT), graphite and graphene as shown in Fig. 7. The mass fraction has significant effects on the thermal properties of the formed PCM composites. As a study conducted by Tao et al. [71] showed, the specific heat capacity and thermal conductivity of PCM composites first increased and then decreased with the mass fraction of carbon nanomaterials rising. Except for carbon nanomaterials, the metal nanoparticles and metal oxide nanoparticles are also used as additives to enhance the thermal conductivity of PCM [72,73]. Metal-based materials possess quite high thermal conductivity as stated previously which is beneficial for thermal conductivity enhancement. However, metal-based materials are not commonly used for medium-high temperature PCM due to their active chemical nature, causing them to be highly reactive with base PCM at high temperatures [25]. Additionally, most of the metal particles and metal oxide particles have a high density, which further restricts their applications.

Except for the thermal conductivity, latent heat is also a crucial thermophysical parameter determining the thermal energy storage performance. Therefore, when adding nanoparticles into the basic PCM, attention should also be paid on the variation of latent heat. In medium-low temperature PCMs, Babapoor and Karimi [74] pointed out that the addition of nanoparticles tended to undesirably reduce the latent. In contract, Rufuss et al. [75] demonstrated by adding copper oxide and titanium oxide into the paraffin improved the latent heat by 15.7% and 64.7% compared with that of the basic paraffin. The reason may be attributed to mechanisms including the effects of nanoparticle concentration, surface charge states of nanoparticles, layering in the solid and liquid interface and the movement of phonons [76]. As for the medium-high temperature PCMs discussed in this review, Zhang et al. [77] demonstrated that the addition of graphene nanosheet into Li_2CO_3-Na_2CO_3-K_2CO_3 decreased the latent heat of basic PCM from 247.1 J/g to 195.6 J/g. Han et al. [78] characterized the thermal properties of composite PCM after adding Al_2O_3, CuO and ZnO into $MgCl_2$-KCl-NaCl with the same concentration of 0.7 wt%, respectively. The results indicated that the latent heat of basic salt was decreased by 2.4%, 6.4 and 7.6% while the addition of Al_2O_3 achieved a much higher improvement of thermal conductivity compared with CuO, and ZnO. Therefore, special attention should be paid to the variation of latent heat when adding nanoparticle additives into the base PCMs to enhance the thermal conductivity, since the existing of nanoparticles may lead to either a reduction or improvement of the latent heat, which depends on the types of nanomaterials, concentrations of nanomaterials as well as the melting-solidification process.

A summary of thermal conductivity enhancement for medium-high temperature PCM with nanomaterial additives is shown in Table 6. It can be concluded that using carbon nanomaterials as additives offers a significant advantage because they possess high thermal conductivity, stable chemical property and low density. The application of carbon nanomaterials should focus on the aspect ratio of different materials since the large aspect ratio of nanomaterials will lead to higher thermal conductivity enhancement. As highlighted, carbon fibres, graphene and carbon nanotubes have a large aspect ratio [25]. The geometrical parameters and mass/volume fraction of nanomaterial also influence the thermal conductivity enhancement, as was investigated by Tao et al. [71]. Also, different preparation and dispersion techniques influence the

Table 5
Summary of medium-high temperature PCM thermal conductivity enhancement with porous media.

Porous media	PCM (m.t./°C)	Method	Remarks	Ref.
Expanded graphite	KNO_3-$NaNO_3$ (222)	Experimental	Reported three different methods to prepare composite materials. The thermal conductivity of composite PCM was improved from 1.1 to 11.7, 40 and 51.5 W/(m K) when the ENG concentrations were 10%, 20% and 30, respectively.	[57]
Expanded graphite	D-Mannitol (164.9)	Experimental	The addition of EG into D-Mannitol leads to remarkable improvement in the thermal conductivity. Specifically, the thermal conductivity of composite PCM increased from 0.60 to 7.32 W/(m K) with the EG concentration of 15%. The storage duration of LTES reduces whilst EG fraction increases.	[60]
Graphite foam	$MgCl_2$ (714)	Numerical	The thermal conductivity of the composite material with graphite foam and $MgCl_2$ as high as 25 W/(m K). Using the newly developed PCM composite material, the roundtrip exergy efficiency in the LTES system significantly improved from 68% to 97%.	[61]
Expanded graphite	$LiNO_3$-KCl (165.6)	Experimental	The thermal conductivities of the composites were 1.85–7.56 times higher compared with the eutectic $LiNO_3$-KCl. The heat transfer performance in the composite material during the heat storage process with EG is better than that without EG.	[62]
Expanded graphite	KNO_3-$NaNO_3$ (222)	Experimental	The highest effective thermal conductivity of salt composite with ENG was 50.78 W/(m K), which was 110 times higher than that of pure salt powder. The additive of ENG-TSA in the PCM caused a slight reduction in latent heat.	[63]
Expanded graphite	$NaNO_3$-KNO_3 (220)	Experimental/ Numerical	The addition of EG significantly enhanced the thermal conductivities, e.g., the thermal conductivities of $NaNO_3$ with 20 wt% EG was measured to be 6.66–7.70 W/(m K), which is about 7 times higher than those of pure $NaNO_3$.	[64]
Graphite foam	NaCl (800)	Numerical	The graphite foam enhanced the overall thermal conductivity of the basic PCM with the potential to considerably improved the heat transfer performance and increase the exergy efficiency of the LTES system.	[65]
Graphite foam	$MgCl_2$ (714)	Experimental	The thermal conductivities of $MgCl_2$/graphite foam composites were significantly higher than those of pure $MgCl_2$ within the measured temperature range. The results also demonstrated that the energy storage density and charging-discharging rate could be controlled by the porosity of the graphite foam.	[66]
Metal foam/ Expanded graphite	$NaNO_3$ (306)	Experimental	The heat transfer rate could be improved by embedding the metal foam, EG and mixture of metal foam and EG by 210%, 190% and 250%, respectively. Results demonstrated the porous structures severely suppressed the natural convection of liquid PCM and then reduced the heat transfer rate.	[67]
Metal foam/ Expanded graphite	$NaNO_3$ (306)	Experimental	Heat transfer performance could be extensively improved by both metal foams and EG, while the charging and discharging period was reduced. Furthermore, the overall performance of metal foams is superior to that of expanded graphite.	[68]
Metal foam	$NaNO_3$ (306)	Numerical	Heat transfer coefficient of the LTES with copper foam could be increased up to 28.1 times in solid-state while up to 3.1 times was achieved in the liquid state. Both the melting and solidification times were significantly shortened.	[69]
Expanded graphite	$LiNO_3$-KCl (166) $LiNO_3$-$NaNO_3$ (194) $LiNO_3$-NaCl (208)	Experimental	The thermal conductivity of different salt compositions impregnated with EG was improved by 4.9–6.9 times within the measured temperature range. The results showed that composite PCMs prepared by impregnation were more homogeneous compared to salt/EG composites prepared by infiltration or compression.	[70]
Metal foam	$NaNO_3$-KNO_3 (220)	Experimental/ Numerical	The temperature difference between the salt and metal foam was distinct due to the high thermal conductivity of the metal skeleton. The natural convection was weakened in the liquid molten-salt with metal foam, while the discharging process was enhanced due to the presence of the metal foam.	[58]

extent of thermal conductivity enhancement as discovered by Nomura et al. [79]. Meanwhile, the preparation methods may affect the homogeneity of formed composite PCMs. Zhong et al. [70] found that the composite PCMs prepared by impregnation were more homogeneous compared to the salt/EG composites prepared by infiltration or compression. A review was conducted by Jurčević et al. [80] to comprehensively analyse the preparation strategies for composite PCMs with nanomaterials. It was concluded that a well-designed preparation method could benefit the rational utilization of nanoparticle additives and reduce adverse environmental footprints released by the production and application of nanomaterial. Therefore, elaboration methods should be carefully identified to achieve the optimal thermal conductivity of the PCM composite adding with nanomaterials.

3. Heat transfer enhancement for medium-high temperature LTES

Except for metallic-based PCMs, other PCMs exhibit low thermal conductivity. which leads to a poor heat transfer process between the PCM and the Heat Transfer Fluid (HTF). Consequently, exploring advanced heat transfer enhancement techniques from the level of the heat exchanger is also important. The most common enhancement techniques involve the use of an extended heat transfer area, heat pipes and layouts of multiple PCMs.

3.1. Extending the heat transfer area

Extending the heat transfer area is the most common and efficient technique to enhance the heat transfer rate between the HTF and PCM due to their simplicity, easy fabrication and low cost [27]. Fins with various shapes and structures are the most frequently used to increase the heat transfer area between the thermal source and PCM and then promote the heat transfer performance of the LTES system [87–95]. In the investigated LTES systems, fins are generally located on the side with relative lower thermal conductivity, which is the PCM in most cases. Taking shell-and-tube LTES as an example, typical configurations of fins with one and two channels are shown in Fig. 8, but fin configurations and geometrical parameters can be varied, including the space, length, number and orientation of fins [96].

Seeniraj et al. [87] investigated the effect of radial fins on the charging performance of a solar LTES unit. Results showed that the fins led to additional heat conduction to accelerate the melting process, but they also caused a non-uniform temperature field near the fins. Agyenim et al. [88] experimentally compared the heat transfer performance of a fin-tube LTES unit employing radial and longitudinal fins. Results recommended the longitudinal fins for a fin-tube LTES because it led to higher heat transfer rate in the charging process and insignificant subcooling in the discharging process. Steinmann et al. [89] conducted an experimental study to investigate the heat transfer performance of a

sandwich-concept LTES unit employing graphite and aluminium fins for solar thermal systems. It was proven that graphite fins were suitable for applications up to 250 °C while aluminium fins were preferred for higher temperature applications. In order to improve the heat transfer performance of $KNO_3/NaNO_3$ eutectic PCM, Bayón et al. [90] also introduced expanded graphite fins into a sandwich configuration LTES for a solar-driven direct steam generation.

Fins can also enhance the temperature uniformity of the LTES. Different fin configurations considering the fin number, fin height and fin thickness were studied to enhance temperature uniformity of a shell-and-tube LTES due to the natural convection of liquid PCM by Tao et al. [97] Results indicated that the fins could enhance temperature uniformity of the melting process and LTES performance at the same time, but the fin parameters should be properly selected and optimized. Tiari et al. [93] also used fins to improve the temperature uniformity of a rectangular container LTES unit shown in Fig. 9. Results revealed the employment of fins provided more uniform temperature distribution, however, it was revealed that smaller fin length led to a narrower temperature difference and the fin number did not have a significant impact on the LTEs performance.

To achieve the optimal heat transfer performance using fins in LTES system, more attention should focus on the selection and optimisation of geometrical parameters. Wang et al. [95] carried out a numerical study to investigate the influence of fin geometrical parameters such as fin length, fin ratio and angle to the adjacent fins on the melting process of a sleeve-tube LTES. Results showed that fin ratio and fin angle were important to accelerate the melting performance while fin thickness has an insignificant effect on the meting process. Elmaazouzi et al. [98] conducted a numerical study to evaluate the effects of fin number (distance) of annular fins on the charging process of a coaxial LTES. The simulation results showed, when respectively inserting 10 fins, 30 fins and 50 fins, the total melting time could be reduced by 31%, 56.5% and 65% compared that of the basic case without fins. It can be found that the total melting time decreased with a smaller rate while the fin number increases. Zauner et al. [94] studied the heat transfer performance of a polyethene PCM storage which was designed for a solar-driven jet ejector chiller plant. Results concluded that increasing fin numbers did not further improve heat storage performance. Fins are also employed in the HTF side to enhance the heat transfer rate between the HTF and tube wall. Tao et al. [91] numerically compared the heat transfer performance of a molten salt LTES system using four different HTF tubes in a solar thermal power plant. Results showed that the three enhanced tubes could reduce the melting time by 19.9%, 26.9% and 30.7% for the dimpled tube, cone-finned tube and helically-finned tube, respectively compared to the smooth tube. Elmaazouzi et al. [99] evaluated the charging performance of a shell-and-tube LTES using annular fins with different length, and it was found that the fin length of 14 mm was the optimal geometry, which was increased the heat transfer rate by 50% at least. The effects of fin length on the heat transfer process of LTES is also affected by other parameters of the system. Yıldız et al. [100] explored the effects of rectangular and tree-like fins with different length in a PV/PCM system on the natural convection behaviour of a molten PCM. The results indicated that the fin length of w/H 0.3 or 0.4 had a negligible effect on the natural convective at low Rayleigh number, but the natural convection showed a remarkable enhancement of 9% when the fin length increased to 0.5.

In summary, future works should focus on the proper selection of fin configurations including the length, width number and angle according to the objective LTES heat exchangers with the potential of achieving the optimal heat transfer performance. However, it should be pointed out that the natural convective heat transfer inside the liquid PCM plays a significant role in the fusion and solidification process, and the application of fins may restrict and even reduce the intensity of convection. Tao and He [97] analyzed the effects of natural convection heat transfer on the charging performance of salt in a horizontal concentric tube. They found that the fins restricted the natural convection in the liquid PCM and the enhancement effects were reduced. Ji et al. [101] also demonstrated that the natural convection could be restricted by fins

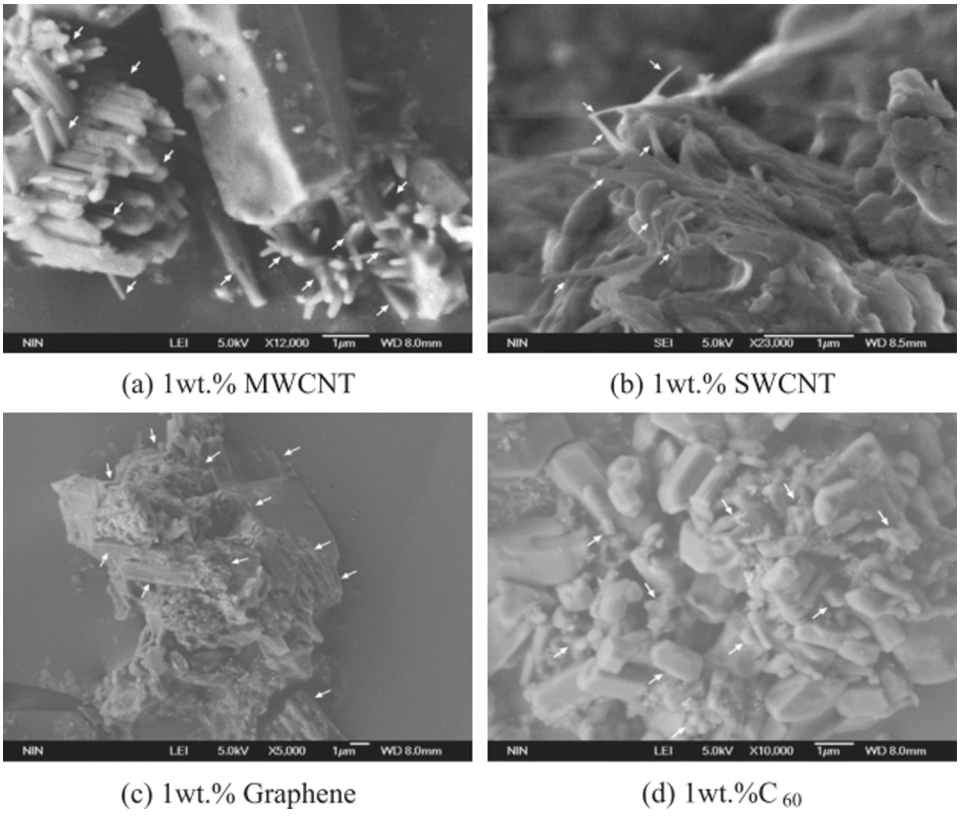

Fig. 7. SEM images of salt composites with different carbon nanomaterials [71].

Table 6
Summary of thermal conductivity enhancement for medium–high temperature PCM with nanomaterial additives.

Nanomaterial additive	PCM (m.t./°C)	Method	Remarks	Ref.
SWCNT, MWCNT, graphene, C_{60}	Li_2CO_3/K_2CO_3 (488)	Experimental	Specific heat capacity and thermal conductivity of PCM composites first increased then decreased with the mass fraction of carbon nanomaterials rising.	[71]
MWCNT	Li_2CO_3-K_2CO_3 (488)	Experimental	The effect of the surface-active agent on the thermal properties of composite PCM had duality. With the mass ratio of SAA to nanomaterial 10:1, PCM thermal conductivity could be increased up to 58.75% by adding 1 wt% MWCNT.	[81]
MWCNT	Na_2CO_3 (851)	Experimental	The thermal conductivity of the composite PCMs increased as the weight fraction of MWCNTs or testing temperature increased.	[82]
Graphite	Polyethene (130)	Experimental	Thermal conductivity was enhanced by the higher mass fraction of graphite. When the mass fraction of graphite was 20 wt%, the thermal conductivity of the PCM increased from 0.51 up to 1.31 W m^{-1} K^{-1}.	[83]
Graphite	KNO_3-$NaNO_3$ (220)	Experimental/ Numerical	Next to the melting point of the PCM, the thermal conductivity intensification factor is 10 for an effective conductivity of 6 W m^{-1} K^{-1}. 40 wt% of graphite was needed to meet the requirement of concentrated solar application	[84]
Graphite	Adipic acid-Sebacic acid (116–150)	Experimental	The supercooling degree of composites could be effectively reduced, and the thermal conductivity of composite PCM was 0.131 W m^{-1} K^{-1} with graphite mass fraction of 0.5%, which increased by 19% compared with pure composite.	[85]
Carbon fibre	Erythritol (118)	Experimental	The effective thermal conductivity of erythritol was increased from 0.73 to 30 W m^{-1} K^{-1} with approximately 25 vol% carbon fibre embedded. Hot-press was more effective than melt-dispersion for preparing high thermal conductivity PCM composite using anisotropic fillers such as carbon fibre.	[79]
Carbon fibre	Erythritol (116.3)	Experimental	The longer carbon fibre showed better performance than the shorter one for thermal conductivity enhancement, which was 3.91 and 2.46 W m^{-1} K^{-1} for longer and shorter carbon fibre at the 10 wt%, respectively. It indicated that the geometry of carbon fibre influenced the thermal conductivity.	[86]
CuO nanoparticles	KNO_3 (334) $NaNO_3$ (306) KNO_3-$NaNO_3$ (222)	Experimental	Significant increase in thermal conductivity was observed for the eutectic salt and pure KNO_3 systems over the entire temperature range, while it was observed only for temperatures under 150 °C for $NaNO_3$ system.	[73]
Al_2O_3 nanoparticles	n.a. (220)	Numerical	LTES with Al_2O_3 nanoparticles achieved a higher melting rate because the thermal conductivity enhancement improved the heat transfer efficiency.	[72]

during the charging process of LTES. The results found that the natural convection was intensified when the length ratio of fins was lower than 1, but the flow motions driven by natural convection became weak when the length ratio was higher than 1. However, the adverse effects of fins on the natural convection is valid only during the melting process of LTES [102]. Therefore, the effects of fins interacting with the convective heat transfer should be considered when determining the geometrical parameters and position of fins.

3.2. Application of heat pipes (HP)

The working principle of HP embedded in LTES system is illustrated in Fig. 10. Due to the phase change heat transfer of working fluid, HP has the potential to significantly increase the melting-solidification process of PCM. HP operates in specific temperature ranges due to the properties of the selected working fluid. There are two categories of HP: wickless (gravity-assisted) and wick assisted (screen mesh) heat pipe [103]. To achieve better matching performance, the operating temperature range, geometrical size and shape of the LTES system play an important role in selecting the suitable shape and designing effective parameters for HP.

Shabgard et al. [104] numerically compared the effects of two different HP layouts on the charging-discharging process of a shell-and-tube based LTES system for solar energy utilization. Two different cases were considered including a configuration with HTF tubes surrounded by PCM and a configuration with HTF passing over tubes containing PCM as shown in Fig. 11. Results demonstrated that a significant increase in the charging-discharging rate of PCM was achieved in both cases. Meanwhile, it was observed that the orientation of HPs in Module 1 had little effect on the charging-discharging performance, while it was an important impact in Module 2. Based on these two layouts, a series of numerical studies were conducted by Nithyanandam et al. [105–107] to investigate the effects of HP geometrical parameters, numbers, orientations on the LTES performance. It was found that the HP effectiveness decreased with the rise of the HTF mass flow rate, module length and tube radius; while it was enhanced by larger length of the condenser section, evaporator section and the vapour core radius for both cases. Also, the optimal number and orientation of HPs exists to achieve the best charging-discharging performance of LTES.

Previous studies focused on HP-PCM with only one channel for HTF, in this configuration, demonstrates that only charging or discharging process is enhanced by HPs. A two-channel layout, as shown in Fig. 12, allows LTES system to operate in different modes: charging (hot HTF flows), discharging (cold HTF flows), charging and discharging simultaneously (hot and cold HTF flows), idling mode (no HTF flows) [108]. The simultaneous charging-discharging mode is important and offers potential for LTES-based waste heat recovery systems. Sharifi et al. [109] numerically investigated the heat transfer mechanism of cylindrical LTES embedded with HPs under simultaneous charging-discharging mode. Results indicated the charging-discharging rate was determined by HP working fluid, conduction in HP wall and wick. Meanwhile, geometrical parameters of the LTES enclosure also played an important role in promoting the melting rate. The simultaneous charging-discharging LTES system can operate in different modes providing a more flexible operation making it suitable for systems of time-dependent energy source, especially solar energy and other renewable energy [110,111].

In addition to the shell-and-tube based HP-PCM system, some researchers focus on the performance of HP-PCM with fins enclosed in a container. For example, Tiari and Qiu et al. [93,112,113] comprehensively investigated the parametric effects on the heat transfer performance of finned HP-PCM systems. Results showed that layout factors including HP arrangement, HP quantities, HP spacing had profound effects on the heat transfer enhancement and thermal response performance of the LTES system. The latest studies are exploring the possibilities of hybrid HP-PCM on industrial applications. Liu et al. [114,115] designed two novel thermal storage units with a gravity-assisted heat pipe. Experimental results disclosed that the proposed thermal energy systems could work isothermally at stable temperatures and showed the potential applications on the solar refrigeration system and other thermal energy storage purposes according to the TES temperature.

Table 7 shows a summary about heat transfer enhancement of medium-high temperature PCM using heat pipes. It can be concluded that there are very limited experimental investigations about the PCM-HPs available. More attention should be focusing on the experimental

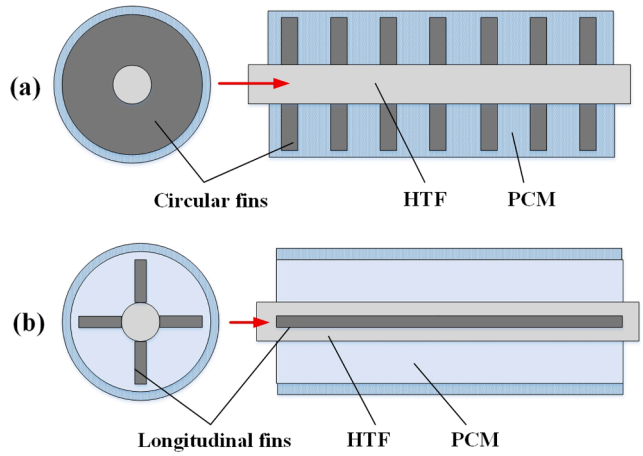

Fig. 8. Schematic diagram of two typical fins for shell-and-tube LTES. (a) Circular fins; (b) Longitudinal fins [88]

work to provide validations and reveal the heat transfer enhancement mechanism of the PCM-HPs. The concept of using LTES with HPs is mainly applied in solar energy utilization. There are very few studies about the application of LTES with HPs to recover fluctuating heat sources including waste heat from industrial process and engine heat recovery. There is a huge potential for two-channel LTES with HPs to recover unsteady heat sources because the charging and discharging process of LTES can simultaneously occur enabling the thermal energy systems being able to operate within the designed conditions. For instance, the PCM-HPs technology can be used by integrating with Organic Rankine cycle as a compact, simple and efficient heat recovery solution.

3.3. Cascaded PCMs

Cascaded PCMs is defined as PCMs with incremental or degressive melting temperature aligned in a linear arrangement. The schematic layout of cascaded PCMs based on the shell-and-tube evaporator is shown in Fig. 13. Generally, there are two types of arrangements of multiple PCMs: multi-PCMs in series and multi-PCMs in parallel. Cascaded PCMs are arranged in decreasing order based on their melting temperature, the heat transfer temperature difference will be larger when the temperature of heat source flow decreases along the flow direction during the charging process, therefore the larger and more stable heat flux can be achieved. In the discharging process, the cold fluid flows into the LTES system in a reverse direction and will be possible to achieve a better heat transfer performance.

A shell-and-tube heat exchanger integrated with five different PCMs is proposed by Gong et al [118]. Five segments of PCMs are arranged in decreasing order according to their melting temperature. Results revealed that energy charging-discharging rate of five PCMs is 34.7% larger than that of a single PCM. It was also highlighted that employing multiple PCMs can effectively reduce the fluctuation of outlet temperature for heat transfer fluids. In Gong's further study [119], the heat transfer performance of the LTES system integrated with single, two, three and five PCMs is compared and optimised from the perspective of exergy efficiency. Results indicated that exergy efficiency of LTES system using three or five PCMs can be one to two times than that of single PCM. Meanwhile, it was concluded that the optimal melting temperatures of multiple PCMs had an approximate relationship with geometrical progression. Li et al. [120] conducted research related to the application of multiple PCMs on solar energy utilisation. The results showed that both the inlet temperature of the heat source and the length of each PCM section had significant effects on the melting times of PCMs. Wang et al. [121] investigated a heat exchanger with the zigzag configuration using multiple PCMs. Results showed that a larger melting temperature difference between the multiple PCMs could lead to more significant heat transfer performance during the charging process, and multiple PCMs with unequal mass ratio could result in further intensification of heat transfer.

Table 8 shows the selected references related to heat transfer enhancement using cascaded PCMs. The majority of studies on the cascaded PCMS are simulation rather than through experiments. Michels et al. [124] experimented to verify the simulation model for studying the performance of different cascaded PCMs-based LTES configurations. The simplified diagram and photo of the test rig are shown in Fig. 14. Experimental results confirmed the positive influence of cascaded PCMs to achieve higher efficiency of energy utilisation and more uniform outlet temperature of HTF. Peiro et al. [126] experimentally compared the performance of single and cascaded PCMs considering indicators such as specific energy stored and heat transfer effectiveness. The LTES tank used to conduct experiments, shown in Fig. 15, is based on the shell-and-tube heat exchanger, where the HTF flows inside the bundle of tubes and PCM is filled outside the tubes. Results showed that cascaded PCMs could achieve an efficiency enhancement of 19.4% and a smaller temperature difference between the inlet and outlet of HTF compared to that of a single PCM. Yuan et al. [122] experimentally compared the thermal performance between the cascaded and non-cascaded high-temperature LTES during the charging, heat preserving and discharging process for solar energy utilization. Experimental results indicated that cascaded LTES system could successfully solve the problem of non-thorough melting of the PCM in the non-cascaded system.

It can be concluded that the application of cascaded PCMs can

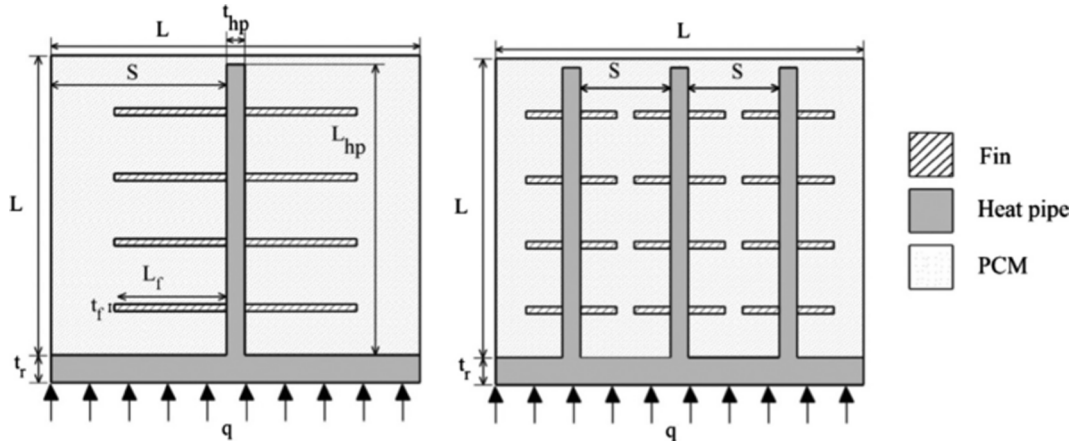

Fig. 9. Schematics of the LTES units with different fin length and fin number [93].

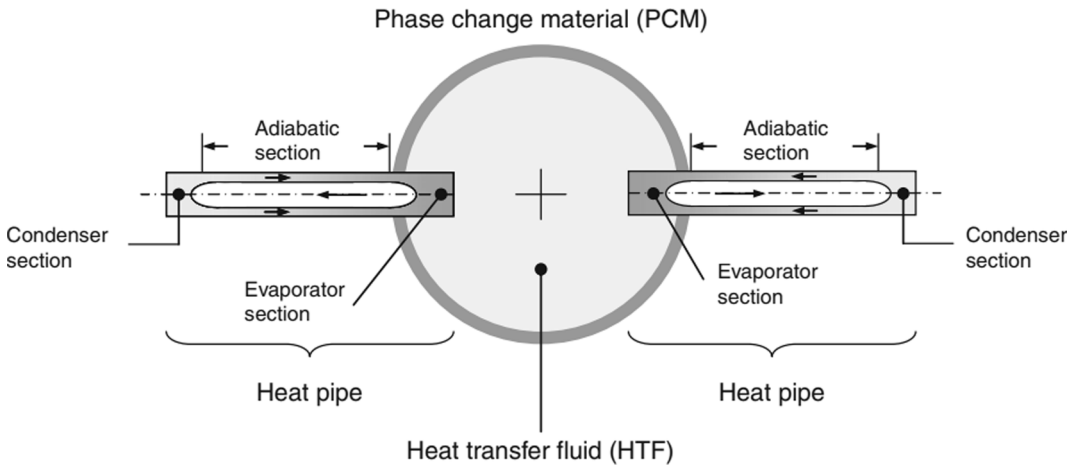

Fig. 10. Schematic diagram of heat transfer between the HTF and PCM using HPs [104].

significantly improve the heat transfer performance of LTES. And the optimal selection of cascaded PCMs in terms of melting temperature plays an important role in the performance improvement of LTES systems. Presently, there are very few investigations into the optimisation of PCM melting temperature for the dynamic heat sources such as industrial waste heat, solar energy and engine exhaust when the cascaded PCMs are employed for waste heat recovering. The fluctuation characteristics of dynamic heat sources, including the period and amplitude, should be paid more attention in future research because they will cause different boundary conditions.

4. LTES in different heat recovery applications

In this section, the LTES using medium-high temperature PCMs in different applications will be reviewed to provide a detailed discussion and information regarding the capability of LTES in real-world

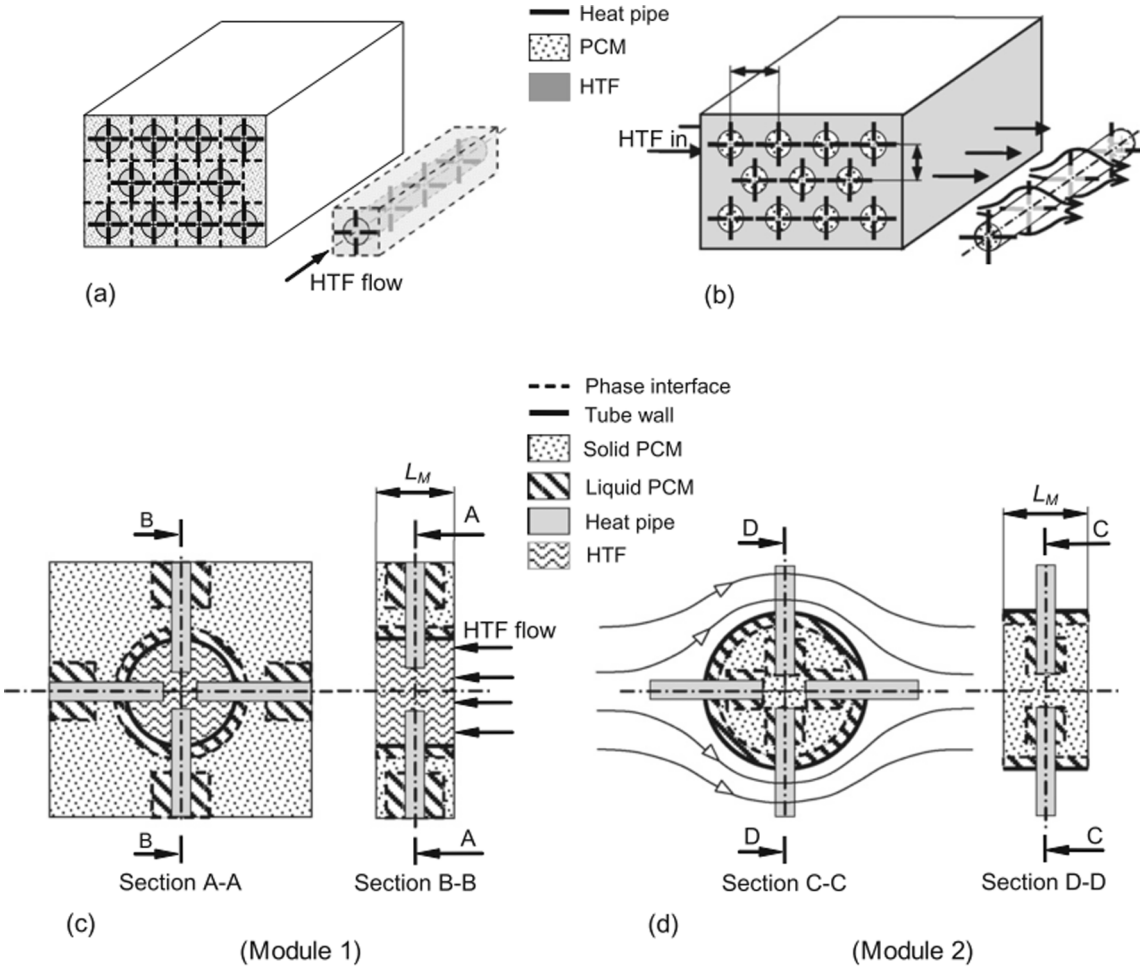

Fig. 11. Two LHTES units: (a) the HTF tubes are surrounded by PCM, (b) the HTF passes over tubes containing PCM, (c) Module 1:a cell unit of (a), (d) Module 2: a cell unit of (b) [104].

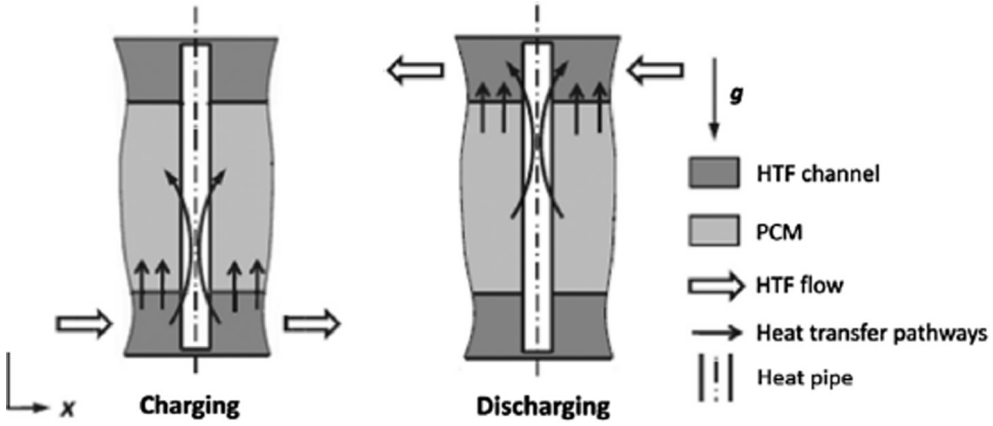

Fig. 12. A two-channel configuration of HP-PCM system during charging and discharging [108].

application to overcome the thermal fluctuating including solar radiation, industrial heat source and engine waste heat. Some representative heat sources such as industrial process thermal and engine waste heat showing the fluctuating and intermittent nature are illustrated in Fig. 16.

4.1. Solar thermal power plants

Because of the large energy storage density of PCMs, combining solar power plants with LTES is the most effective method to provide flexible electricity to the grid and supply large-scale power services. Hence, the applications of LTES in solar thermal power plants have been widely explored and developed in the last ten years. Most of the existing studies concentrate on the parametric study and economic evaluation of the system, due to the difficulty of large scale installation and complexity of the solar thermal power system coupling LTES. Guo et al. [134] conducted a parametric study for a typical simplified solar power system using a finned multi-tube high-temperature LTES as shown in Fig. 17. Results demonstrated the effectiveness of using fins to improve the thermal conductivity of salt composition during the discharging process, but the fin thickness and distance should be optimized to achieve improved discharging performance. Robak et al. [135] conducted an economic evaluation of an LTES system for large-scale solar power plant applications based on the energy and exergy analysis. Results indicated that a potential 15% reduction in capital cost of the proposed LTES-based system might be achieved compared to the conventional system using sensible latent heat storage. Mahfuz et al. [136] analysed the energy and exergy performance of a solar power plant to explore the possible improvement of the current solar power plant integrating with LTES. It was found that overall exergy efficiency is about 10% without LTES. In contrast, around 30% overall exergy efficiency could be obtained for the solar power plant coupling LTES, which demonstrated the superiority of the application of LTES in solar power plants.

Casati et al. [137] proposed a simple direct evaporating solar power system, in which the ORC working fluid extracted heat directly from LTES without additional HTF (see Fig. 18). Results of a case study showed that an estimated efficiency of 25% could be achieved, corresponding to a value of 18% under-designed working conditions for the conventional system. Freeman et al. [138] developed the stated direct coupling system as a combined solar heat and power system. Results demonstrated that PCM was the most efficient TES material compared with other sensible TES materials such as water and rocks in terms of power output and working duration. Under the PCM-based layout, the authors highlighted that the melting temperature and volume of PCM, as well as the LTES geometrical parameters, should be paid additional attention. Li et al. [139] discussed the dynamic performance of a small-scale solar ORC system with LTES including the solar disturbance. The effects of LTES volume, solar fluctuation conditions including the amplitude and period, as well as the ORC evaporating temperature were studied. According to the results, a resonance phenomenon was found between solar disturbance and system thermal inertia.

Other studies focused on the experimental test of the solar power system coupling LTES. Laing et al. developed a storage module (see Fig. 19) with $NaNO_3$ and steam as PCM and HTF [140]. The module was operated for 172 cycles (more than 4000 h) from 296 °C to 316 °C, and it was proved that no decomposition of the salt PCM and no degradation of the steam tubes occurred. Then the storage module was used in a large scale unit as shown in Fig. 20 by Liang et al. [141]. The storage unit was

Table 7
Selected references about heat transfer enhancement for LTES using heat pipes.

HP material/working fluid	System configurations	Research approach	Effects of HP number/ orientation	PCMs (melting temperature/°C)	Ref.
Stainless steel/Mercury	Shell-and-tube	Numerical	Included	KNO_3 (335)	[104]
Stainless steel/Mercury	Shell-and-tube	Numerical	Included	KNO_3 (335)	[105,106]
Stainless steel/Mercury	Shell-and-tube	Numerical	Included	KNO_3 (335)	[105,106]
Stainless steel/Biphenyl	Shell-and-tube	Numerical	Not Included	NaOH-NaCl (370). KCl-$MnCl_2$-NaCl (350), NaOH-NaCl-Na_2CO_3 (318)	[108]
Stainless steel /Sodium	Cylindrical	Numerical	Not Included	Cu-0.3Si (803)	[109]
n.a.	Cylindrical	Numerical	Included	$NaNO_3$-KNO_3 (220)	[112]
n.a.	Cylindrical	Numerical	Included	KNO_3 (235)	[93]
n.a.	Cylindrical	Numerical	Included	KNO_3 (235)	[113]
Stainless steel /Water	Cylindrical	Experimental	Not Included	Mixture of RT100 and HDPE (70–120*)	[114]
Stainless steel /Naphthalene	Cylindrical	Experimental	Not Included	$NaNO_3$-KNO_3 (200–250*)	[115]
Stainless steel /Sodium	Cylindrical	Numerical	Not Included	80.5LiF-19.5CaF2 (767)	[116]

* Range of melting temperature.

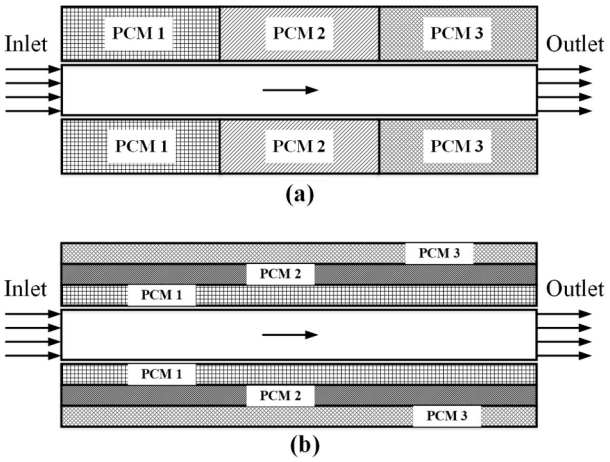

Fig. 13. Different arrangements of multiple PCMs: (a) multi-PCM in series; (b) multi-PCMs in parallel [117].

combined with two sensible thermal energy storage and was used in a direct steam generation system. After tests of 172 cycles under the melting temperature, no degradation was observed, which demonstrated the feasibility of the sandwich-concept storage unit to enhance the heat transfer efficiency and power density during the discharging process. Bayón et al. [90] also tested a sandwich-concept LTES prototype for solar steam generation systems under real operating conditions. The test results under a selected day showed that the obtained thermal power output was lower than the designed value as a result of the excess PCM mass and thermal insulation. A novel reflux LTES system for generating high-temperature superheated steam was developed and tested to extend the operating time of solar thermal-to-electric systems by Adinberg et al. [142]. In this system, the Zn-Sn alloy was used as PCM. The test results indicated the superiority of the Zn-Sn PCM compared with commonly used molten salts since the developed system had outstanding chemical stability and heat transfer performance despite the high cost of metal alloys.

4.2. Industrial waste heat recovery

An excess amount of waste heat generated by different industrial processes is usually dissipated into the environmental atmosphere. Table 9 shows the potential amount of industrial waste heat for some industrialised countries. There is significant potential for industrial waste heat in these countries. For example, industrial waste heat accounts for 26.4% and 17.4% per energy consumed in Canada and Turkey. While industrial waste heat consumed by the USA is only 1.4% of the energy consumed by the country. It means there is still a huge potential to use industrial waste heat in developed and developing countries. Table 10 shows the temperature range of exhaust gases and the high temperatures show the potential for industrial waste heat recovery.

In previous decades, the applications of LTES, using medium-high temperature PCMs in industrial waste heat recovery, have been underestimated since there are very limited studies focusing on this topic. Table 11 shows a summary of the LTES system using medium-high temperature PCMs in industrial waste heat recovery applications. As early as around 2000 s, Maruoka et al. [145–148] conducted pioneer studies to explore the feasibility of using metal balls coated with nickel as PCM to recover high-temperature waste heat produced by plants of chemical productions and steelmaking. Boer et al. [149] developed an LTES-based system using an assumed metal PCM to recover the waste heat of the industrial batch process. The techno-economic evaluation indicated that the presence of the LTES heat recovery system could save 50–70% of the heat for the batch reactors.

Table 8
Selected references for heat transfer enhancement with cascaded PCMs.

System configurations	Research approach	Stages of PCMs	PCMs (melting temperature/°C)	Ref.
Shell-and-tube	Numerical	5	Hypothetical (767, 717, 667, 617, 567)	[118]
Shell-and-tube	Experimental	3	Li_2CO_3-K_2CO_3 (35–65*, 500), Li_2CO_3-K_2CO_3 (47–53*, 484) Li_2CO_3-K_2CO_3-Na_2CO_3 (22–62–16*, 422)	[122]
Shell-and-tube	Numerical	3	KF-CaF_2 (1–15*, 779) KF-CaF_2 (80.5–19.5*, 767), KF-CaF_2 (1–60*, 717)	[123]
Shell-and-tube	Numerical	3	K_2CO_3-Na_2CO_3 (51–49*, 710), Li_2CO_3-Na_2CO_3-K_2CO_3 (20–60–20*, 550), Li_2CO_3-K_2CO_3-Na_2CO_3 (32–35–33*,397)	[120]
Shell-and-tube	Numerical/ Experimental	5	$MgCl_2$-KCl-NaCl (60–20–20*, 380), KOH (360), KNO_3 (335), KNO_3-KCL (95.5–4.5*, 320), $NaNO_3$ (306)	[124]
Shell-and-tube	Numerical/	5	KF-CaF_2 (80.5–19.5*, 767), LiF-MgF2 (1–1, 735), Hypothetical (700, 650, 600)	[87]
Shell-and-tube	Numerical	3	Hypothetical (525, 425, 290)	[125]
Shell-and-tube	Experimental	2	Hydroquinone (165–172&), D-mannitol# (155–162&)	[126]
Shell-and-tube	Numerical	3	NaOH-NaCl (370), KCl-$MnCl_2$-NaCl (350), NaOH-NaCl-Na_2CO_3 (318)	[108]
Shell-and-tube	Numerical	3	LiF-CaF_2 (80.5–19.5*,767), K_2CO_3-Na_2CO_3 (51–49*, 710), LiF-MgF_2(67–33*, 742)	[127]
Zigzag-plate	Numerical	3	Hypothetical (460, 440, 420) %	[121]
Packed-bed	Numerical	3	Li_2CO_3-K_2CO_3 (35–65*, 505), $MgCl_2$-NaCl (55–45*, 440), $MgCl_2$-KCl-NaCl (60–20-20*, 382)	[128]
Packed-bed	Numerical	3	KNO_3 (330), NaOH (318), $ZnCl_2$ (280)	[129]
Packed-bed	Numerical	3, 5	NA (375), NA (340), NA (305) and NA (375), NA (360), NA (320), NA (305)	[130]

* Mass ratio.
& Range of melting temperature.
# δ-phase.
% Only one case is presented.

In the last five years, Magro et al. [2,150–154] conducted a series of numerical studies related to the industrial waste heat recovery systems adopting LTES, considering the thermal power fluctuation of industrial exhaust gas. Firstly, the authors designed a buffering system and PCM container (see Fig. 21) to reduce the fluctuation of exhaust gas temperatures and thermal power for electric arc furnaces [150,151]. Results indicated the temperature and thermal power fluctuation of the exhaust gas at the outlet of the proposed buffering system were effectively reduced, leading to high thermal efficiency for downstream Rankine cycle system. Later, the authors numerically analysed the thermal stress of the previously proposed PCM container under the working temperature [152]. This study revealed the importance of selecting the proper encapsulating materials for PCM and geometrical parameters for the

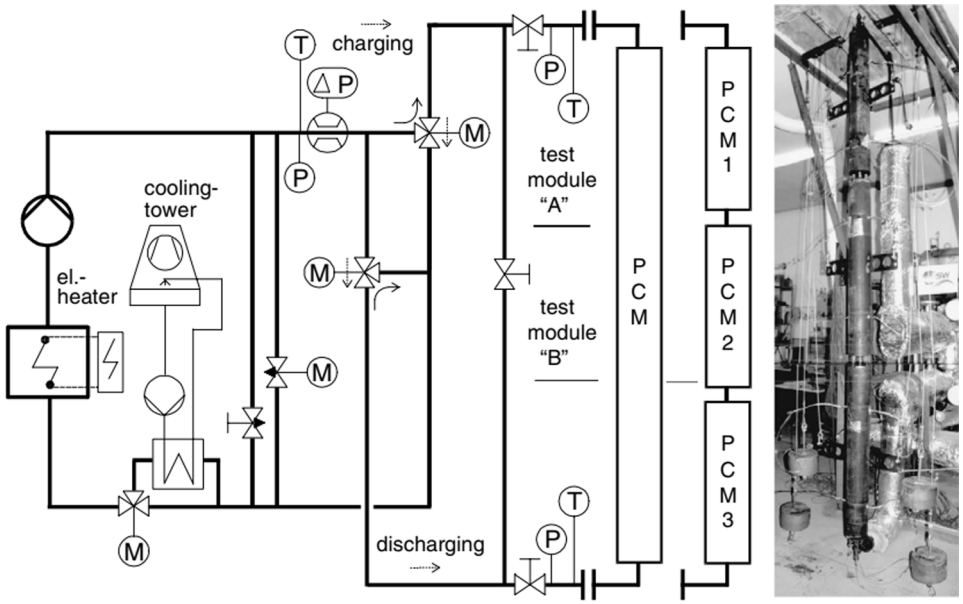

Fig. 14. Simplified schematic diagram of the test facility. The photo on the right side shows test module ''B'' before the test modules were insulated [124].

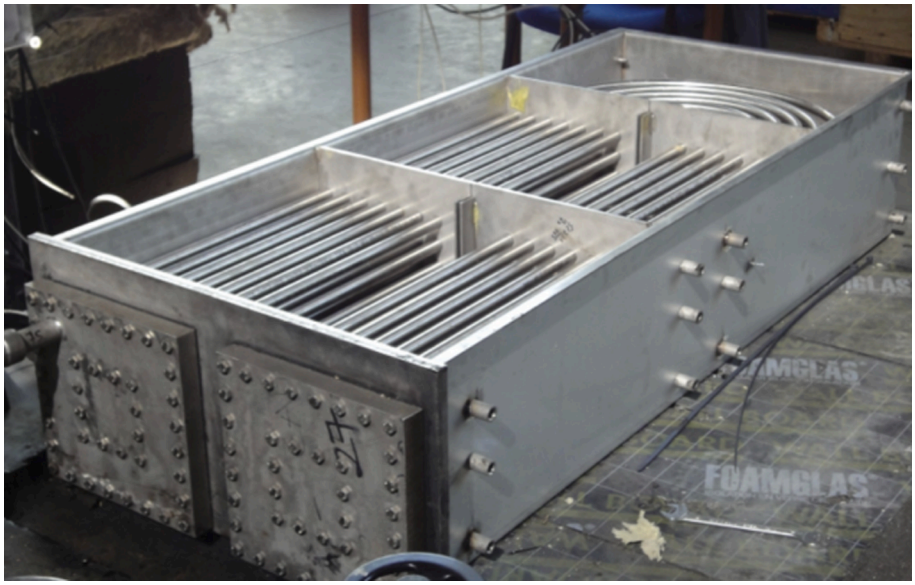

Fig. 15. Picture of an LTES tank for experimental investigation [126].

container. After the specification of the PCM container, the authors focused on the performance analysis and optimization of the whole recovery system integrating with LTES, and compared the heat recovery performance between the conventional system and proposed PCM-based system (see Fig. 22) [2,153]. Results based on thermodynamic analysis showed that introducing the proposed PCM-based technology into the current WHR system allowed the capacity factor of ORC unit to rise from 38% to 52% and the average thermal efficiency to rise from 15.5% to 16.4% [2]. The authors also introduced PCM-based technology into a superheated steam generation system recovering the waste heat of the steel industry [153]. The thermodynamic and economic analysis revealed that the size of the steam generator and the turbine could be decreased by 41% compared to the conventional system. Finally, the authors developed a novel TES device combining high-temperature PCM and bricks to mitigate the steam production fluctuation and improve the efficiency of waste-to-energy plants [154].

It can be concluded that the PCM type has a crucial impact on the design and performance of component-level heat exchanger, which should match the heat source and the objective application. Additionally, for high-temperature PCMs, the selection of proper encapsulating materials also should be addressed since the failure of the container may lead to leakage damaging the system. From the perspective of system level, the design of the LTES unit, the combination of the LTES unit and conventional WHR system requires more attention. From Table 11 it can be seen that almost all the related studies are numerically investigations apart from a few pieces of research about PCM preparation and cycling test. Therefore, conducting more experimental studies is urgent and crucial to obtain a deeper insight into the implementation of PCM-based system in industrial waste heat recovery.

It should be noted that the above-described studies are all focusing on the on-site applications of industrial waste heat using LTES systems. In recent years, off-site applications of industrial waste heat recovery using transportable LTES systems have been attracting increasing attention, because the excess waste heat can be stored by LTES unit and

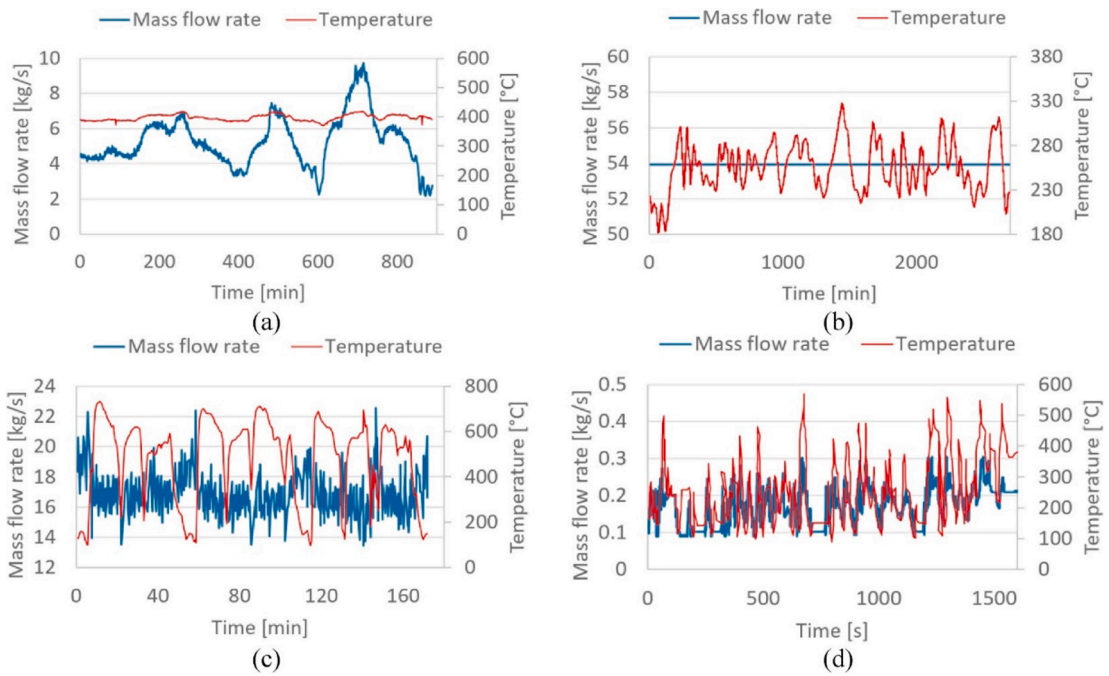

Fig. 16. Variations of temperature and mass flowrate of some typical thermal sources in industrial processes and engines [3]: (a) Steel billet reheating furnace: mass flow fluctuations [2]; (b) Clinker cooling: temperature fluctuations [131]; (3) Electric arc furnace (after water cooling system): fluctuations of both mass flow and temperature [132]; (4) Internal combustion engine exhaust: fast fluctuations [133].

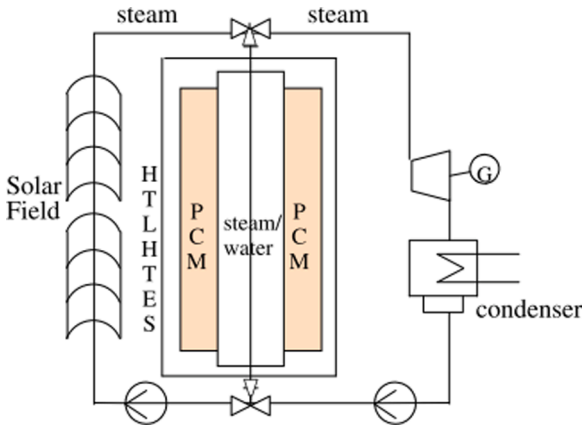

Fig. 17. Schematic diagram of the simplified solar power system using LTES [134].

used later in other locations and applications. A typical transportable LTES waste heat recovery system proposed by Takuya Nagumo et al. [155] is shown in Fig. 23. Recent advancements on transportable LTES can be found in the review articles [13,22,156] and references [157–164].

4.3. Engine waste heat recovery

When investigating waste heat recovery of engines, LTES using low-temperature PCMs have been explored to improve the cold-start performance [166,167]. In contrast, little attention has been given to the applications of LTES using medium-high temperature PCMs in recovering waste heat of engine exhaust gas.

From a general point of view and without considering specified applications, several different experimental and numerical studies were conducted to explore the charging-discharging performance and suitable configuration of LTES coupled with a diesel engine [168–171] based on the same layout (see Fig. 24). Gopal et al. [168] conducted an energy and exergy analysis of a coupled system of LTES and a two-cylinder diesel engine under different operating loads. The engine coolant was taken as the heat source with the temperature of 80 °C and the paraffin was used as PCM. Results showed that the energy efficiency of the integrated system varied from 3.19% to 34.15% while the exergy efficiency ranged from 0.25% to 27.41%, which indicated that both the PCM and HTF should have higher working temperatures in order to minimise heat loss. The following two studies conducted by Pandiyarajan et al. [169,170] employed castor oil and paraffin as HTF and PCM, respectively. In this two studies, the charging experiments were conducted under different engine operating conditions including 25%, 50%, 75% and full load, and the exhaust temperature reached about 160 °C, 250 °C, 280 °C and 350 °C, respectively. Results showed that up to 15.2% of fuel could be saved compared with the same setup without the LTES system. These studies also pointed out the significance of selecting proper PCM and HTF to match the heat source temperature, as well as the potential increased efficiency of using a cascaded LTES layout. Based on previous single-LTES system, Chinnapandian et al. [171] continued to study the double-LTES system, in which d-sorbitol and paraffin were used as PCMs and arranged in cascaded layout. The engine working conditions were identical to the above two studies and the temperature of engine exhaust was also set as 160 °C, 250 °C, 280 °C and 350 °C under four different conditions. It was observed, based on experimental results, that the total recovered waste heat of the double-LTES system was improved up to 20% in contrast to the single-LTES system. Prabu and Asokan [172] conducted experimental work based on the same layout and the same engine operating conditions, but the cylindrical capsules were replaced by spherical containers for PCM encapsulation. The polyethene and water were selected as PCM and HTF, respectively. The experimental results showed that recovered heat accounted for about 7% of the total exhaust waste heat. The above studies preliminarily investigated the energy storage performance of LTES taking the engine coolant and exhaust as heat source without considering the specific applications, which demonstrated the feasibility and high efficiency of coupled LTES-engine system. The proposed system prototype is potential to be applied in the future LTES-based heat recovery system.

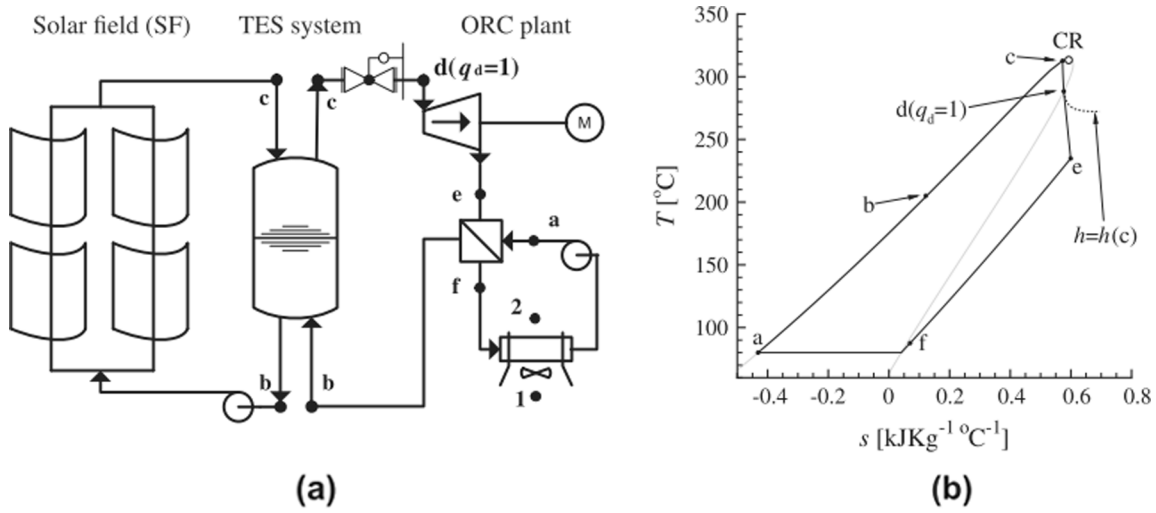

Fig. 18. (a) Simplified layout of a solar plant-LTES-ORC system; (b) T-s diagram of ORC unit [137].

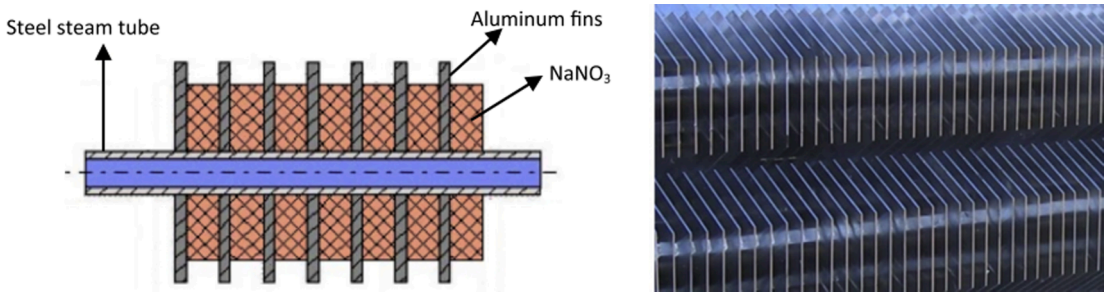

Fig. 19. Schematic diagram of $NaNO_3$ module with steel fins for solar power plants [140].

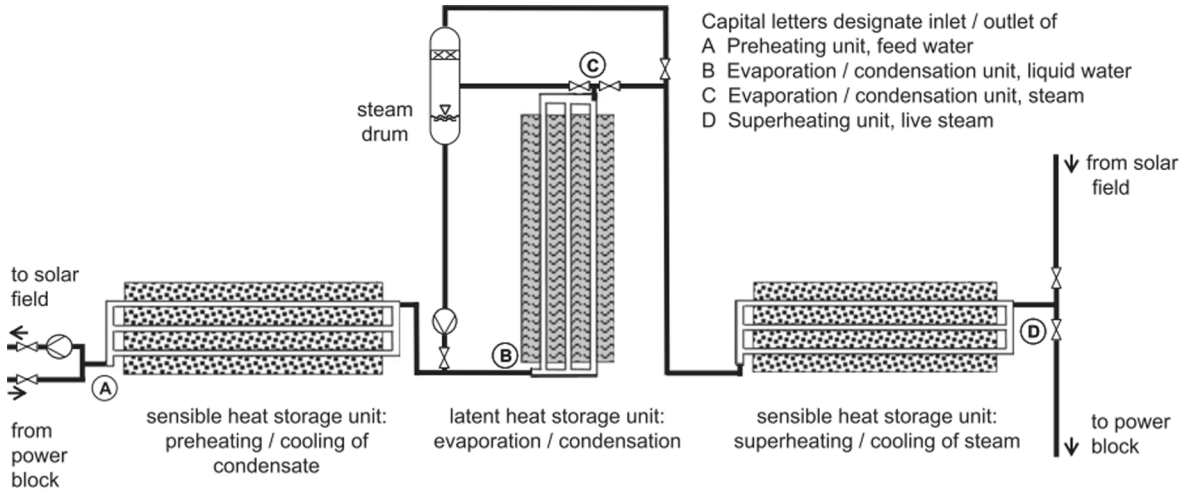

Fig. 20. Overview of the proposed three-part storage unit for solar steam generation system [141].

As for specification applications of LTES in engine waste heat recovery, Jungwook Shon et al. [173] proposed an LTES system using xylitol as PCM to recover the waste heat of engine coolant, and the temperature of coolant was set as about 100 °C according to the conventional engine driving conditions. The recovered heat was used to quickly increase the temperature of the engine during the cold-starting process. The results showed that the warm-up time was reduced by 33.7%. In order to mitigate the thermal power fluctuation of exhaust gas, Yu et al. [174] proposed an organic Rankine cycle system integrating with double latent thermal energy storage to recover the waste heat of engine exhaust gas as shown in Fig. 25. In this study, a real temperature profile of engine exhaust was adopted as a heat source at the temperature range of about 200–400 °C. This pioneering work used salt compositions as PCMs, and twelve salt compositions were screened in detail. Results demonstrated that the fluctuation of the engine exhaust heat can be potentially overcome by the proposed solution. Additionally, the effects of LTSE volume and layouts established that ORC can be combined with double LTES delivered 17.2% greater total power output than that of single LTES under the same LTES volume and operational conditions.

Table 9
Industrial waste heat potential in selected counties [143].

Country	Industrial waste heat potential (EJ)	Total industrial energy consumption (EJ)	Industrial waste heat per energy consumed by industry (%)	Total country energy consumption (EJ)	Industrial waste heat per energy consumed by country (%)
USA	11.5	37.9	4	102.6	1.4
EU	2.7	12.2	22.2	48.2	5.6
Canada	2.3	3.2	71	8.7	26.4
Turkey	0.857	1.8	46.9	4.9	17.4
Japan	0.59	5.7	1	13.3	0.4
Korea	0.384	5.3	8	8.1	4.7

Table 10
Temperature range of exhaust gas from typical industrial processes [144].

Industrial process	Temperature of exhaust gas
steam boilers	~480 °C
gas turbines	~540 °C
cement kilns	~620 °C
copper refining furnaces	~820 °C
aluminium furnaces	~1200 °C
glass melting furnace	~1540 °C
iron and steel furnace	~1550 °C
drying	70–120 °C
boiling	~105 °C
cooking	~115 °C
sterilising	~130 °C
steaming	~130 °C

When the LTES using medium-high temperature PCMs is considered for waste heat recovery of engine exhaust and coolant, the matching of PCM melting temperature and heat source temperature is quite important. Generally, the temperature of engine coolant is between 80–100 °C, and the coolant loop is generally pressurized to maintain the coolant in the liquid phase with the antifreeze boiling temperature being just above 120 °C. According to Table 1, some organic PCM with melting temperature lower than 120 °C such as RT 100 (100 °C), Dimethyl fumarate (102 °C) and Oxalic acid (105 °C) can be selected. In addition, there are a large number of organic PCMs and salt hydrates with the melting temperature at the range of 60–100 °C [175,176]. As for the temperature of engine exhaust, it is generally between the 200–800 °C for diesel and gasoline engines shown in Fig. 26 [177], therefore, salt and salt composite listed in Table 3 and metallic materials listed in Table 4 can be carefully selected according to the requirements of objective heat recovery systems and cost.

5. Conclusions

This paper presents a comprehensive review of the recent developments the applications and technological challenges for heat recovery, storage and utilisation with latent thermal energy storage from the material-level, component level and system-level perspectives. The analysis of the existing literature has demonstrated the feasibility of using LTES as a buffer to balance the thermal power fluctuation from different heat sources, as well as match the energy supply and demand in time and space aspects. Main findings and future potential prospects of this topic are concluded as follows:

(1) Medium-high temperature PCMs mainly include some organic compounds, inorganic salt and metallic materials, which possess quite different thermophysical properties. For organic materials, sugar alcohols have a higher melting temperature and latent heat as well as greater supercooling. For pure inorganic salts, they are high in working temperature, thermal stability, and specific heat. The eutectic salts provide additional options to modify the thermophysical properties of pure salts. However, the prediction of thermophysical properties for salt compositions is challenging because of the lack of experimental data. Composites with lithium salts have been emerging as important options since they can reduce the melting temperature, expand the working temperature and promote thermal stability. As for metallic materials, although they have high thermal conductivity and energy storage capacity per volume unit, they have not been widely applied as

Table 11
Summary of LTES system using medium-high temperature PCMs in industrial waste heat recovery applications.

Year	Industrial sector	Research method	Waste heat source	Heat source temperature	PCM (M.t./°C)	Heat recovery method	Objective applications	Ref.
2002	Chemical products	Experimental	Exhaust gas	1127–1527 °C	Copper ball (1083)	Endothermic reaction	Methane reforming reaction	[145]
2003	Chemical products	Experimental	Exhaust gas	328–727 °C	lead pellets (328)	n.a.	n.a.	[146]
2004	Steelmaking	Numerical	Exhaust gas, Molten slag	Over 1500 °C	Copper ball (1083)	Endothermic reaction	Methane reforming reaction	[147]
2006	Steelmaking	Numerical	Exhaust gas	1300 °C	Copper ball (1083)	Endothermic reaction	Methane reforming reaction	[148]
2006	Chemical products	Numerical	Chemical reactants	180 °C	Metal ball (140)	Rankine cycle	Preheating of reactants	[149]
2010	Steelmaking	Experimental	Exhaust gas	over 1000 °C	Copper ball (1083)	Endothermic reaction	Methane reforming reaction	[165]
2014	Electric arc furnaces	Numerical	Exhaust gas	223–950 °C	Aluminum (660)	Rankine cycle	Electrical energy generation	[150]
2015	Electric arc furnaces	Numerical	Exhaust gas	300–958 °C	Aluminum (660)	Rankine cycle	Electrical energy generation	[151]
2016	Electric arc furnaces	Numerical	Exhaust gas	200–958 °C	Aluminum (660)	n.a.	n.a.	[152]
2017	Billet reheating furnace	Numerical	Exhaust gas	Average of 850 °C	Al-12 wt% Si (576)	Organic Rankine Cycle	Electrical energy generation	[2]
2017	Electric arc furnaces	Numerical	Exhaust gas	390–990 °C	Al-12 wt% Si (576)	Rankine cycle	Electrical energy generation	[153]
2018	Waste to energy plants	Numerical	Exhaust gas	400–850 °C	Aluminum (660) Al-12 wt % Si (576)	Rankine cycle	Electrical energy generation	[154]

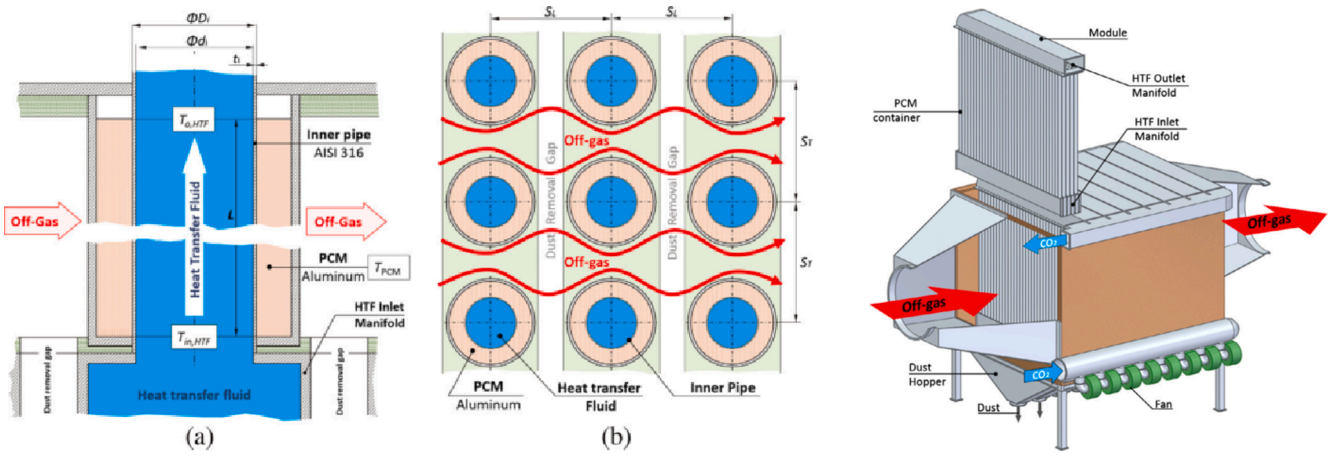

Fig. 21. Schematic diagram of the PCM container: (a) side view; (b) top view; (c) space diagram [151].

PCMs except for some ultra-high temperature situations because of the high density, high cost and lack of experimental data for alloys.

(2) The commonly used thermal conductivity enhancement techniques are adding porous media and nanoparticles into base PCMs. For the former one, metal foam and expanded graphite are the most extensively selected porous media. As for adding nanoparticles, both metallic particles and carbon-based nanomaterials attract the most attention. No matter which techniques are used, the thermal conductivity of PCMs can be substantially

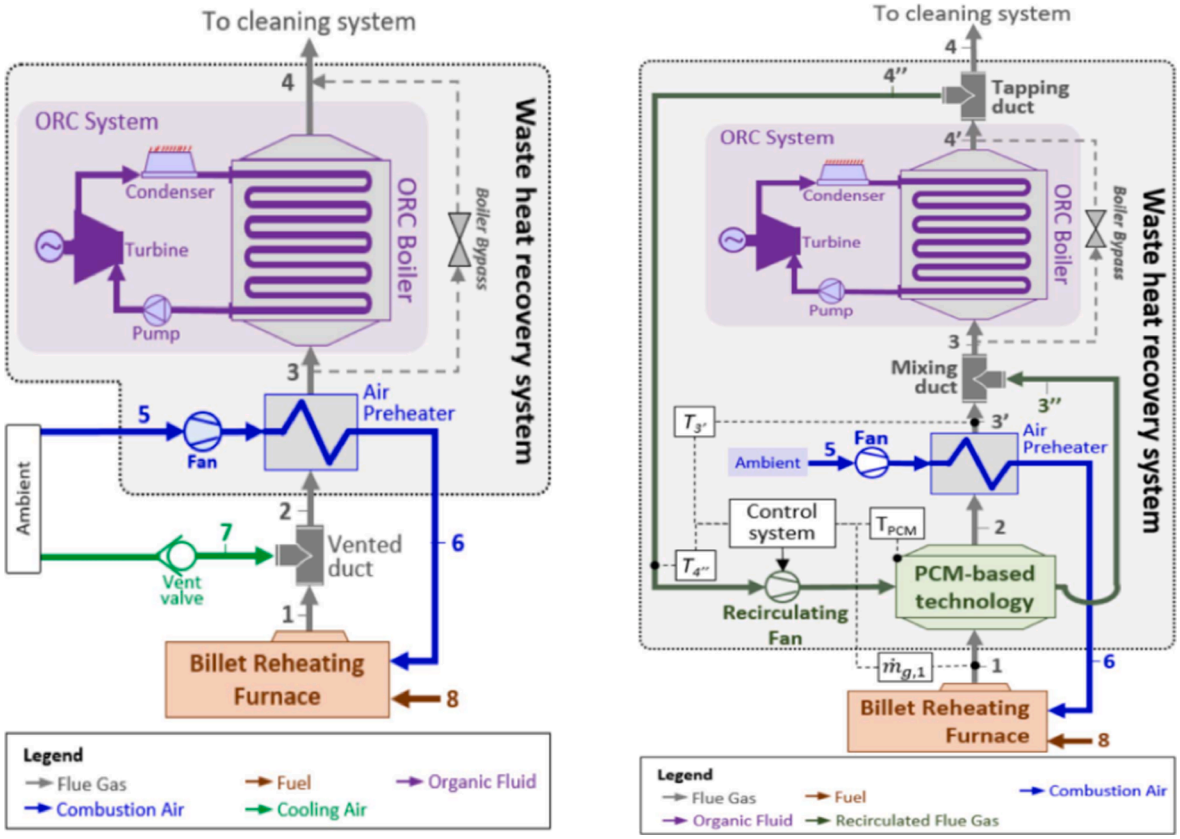

Fig. 22. Comparison of two WHR systems: (a) current system; (b) PCM-based system [2]

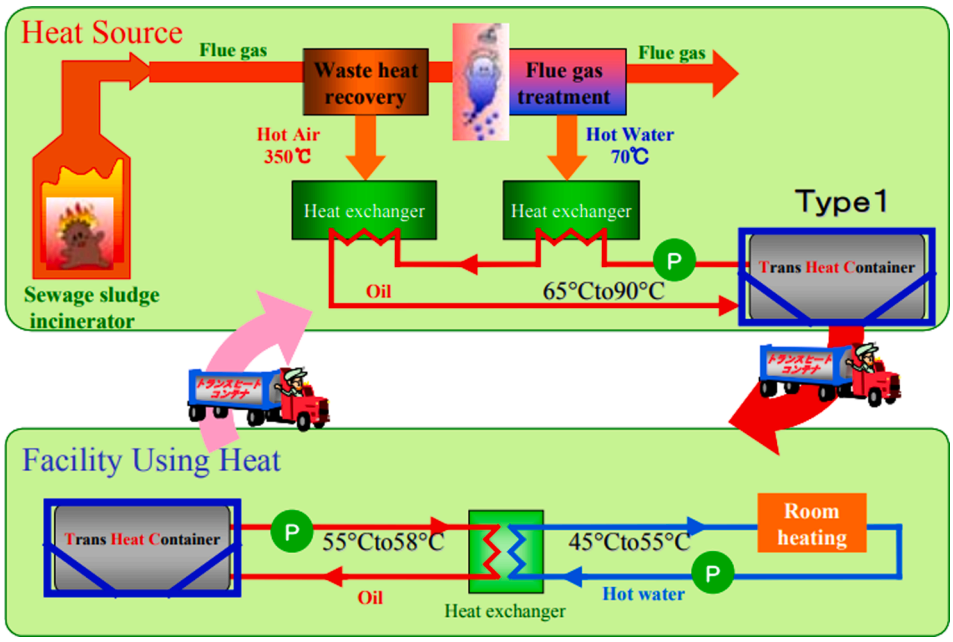

Fig. 23. Flow diagram of a typical mobilised LTES heat recovery system [155].

improved. Nevertheless, it is worth noting that all the additives have adverse effects on the natural convection of liquid PCM during the melting process. The mass/volume fraction of additives need to be carefully investigated in order to find a trade-off between the thermal conductivity enhancement and natural convection restriction. Additionally, different preparation and dispersion techniques influence the extent of thermal conductivity enhancement, which should be given more attention in future investigations.

(3) As for heat transfer enhancement, fins are a simple and efficient method for LTES systems. However, the adoption of fins will reduce the PCM volume and weaken the natural convection of liquid PCM, causing the reduction of thermal storage capacity and heat transfer rate. Therefore, more attention should be given to fin patterns, fin geometries and fin numbers in future research. Heat pipes have been another open research area for heat transfer enhancement in recent years since the phase change heat transfer of working fluids can significantly augment the melting-solidification process of PCMs. Future works should focus on the experimental validations and the ability to design heat exchanger geometries for hot and cold sides of heat pipes. The technique of using multiple PCMs can improve the heat transfer rate and temperature uniformity of the LTES systems. However, this technique significantly depends on the ratio of PCMs and thermal properties. Future studies on the selection and matching criteria of multiple PCMs are crucial for cascaded LTES systems.

(4) In terms of the applications in different heat recovery systems, the first core problem is to select the PCM with proper melting temperature according to the objective application. In addition, packaging the PCM requires balancing a number of potentially conflicting factors. LTES has to provide an adequate heat transfer rate between the heat source and PCM, as well as PCM and HTF,

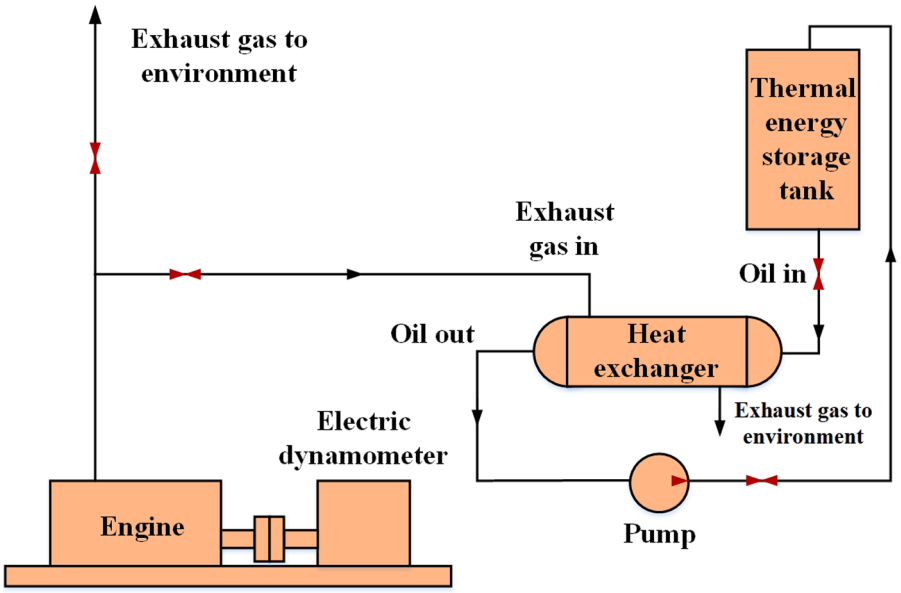

Fig. 24. Schematic diagram of the LTES and diesel engine coupling system [169].

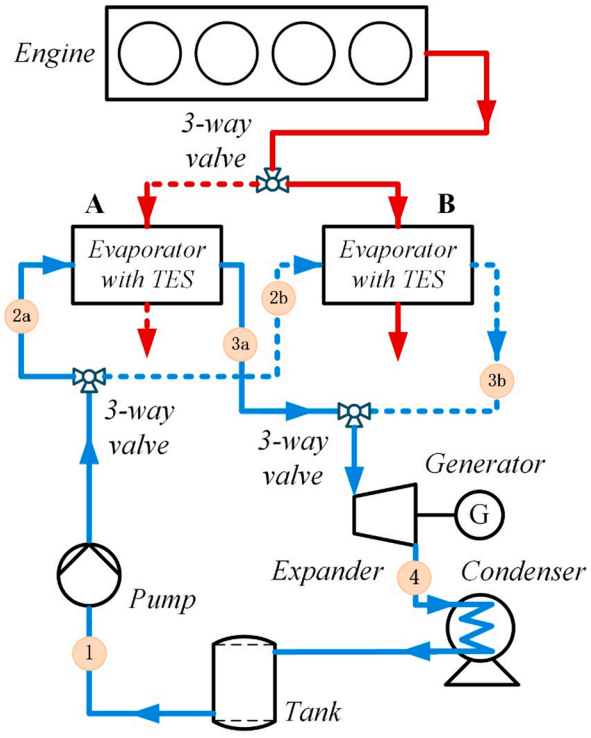

Fig. 25. Schematic diagram of the ORC integrated with double latent thermal energy storage [174].

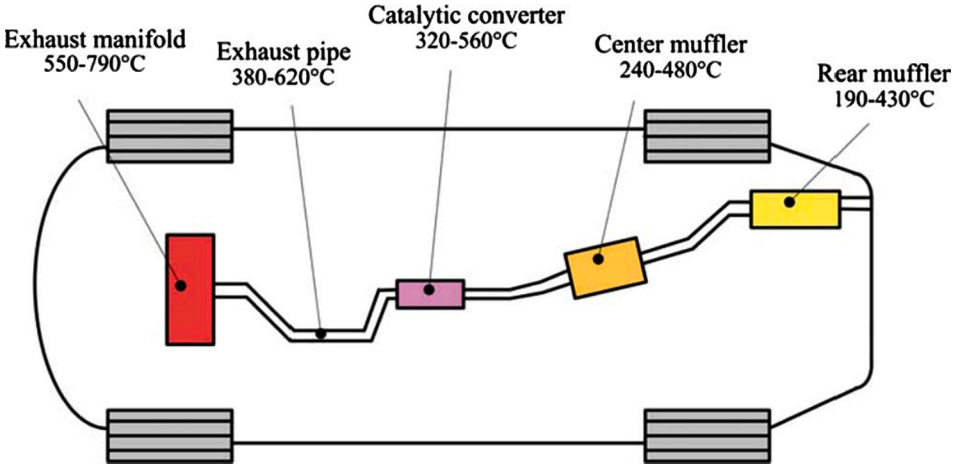

Fig. 26. Range of available exhaust temperatures in a passenger vehicle [177].

overcoming the typically low thermal conductivity of most PCMs during the charging-discharging process. Conversely, it will have to maintain proper PCM form of both solid and liquid state, despite the potentially significant PCM volume change over numerous repeated cycles. Finally, the solution must satisfy the limitations in the size, weight and cost which can be tolerated on by the objective system. While solutions to the individual problem may be easily available, finding an effective comprehensive solution for different systems poses a tremendous engineering challenge.

Declaration of Competing Interest

The authors declare that they have no known competing financial interests or personal relationships that could have appeared to influence the work reported in this paper.

Acknowledgements

This research received support from the Royal Academy of Engineering through the Transforming Systems through Partnerships program (Grant No. TSP1098), the EPSRC grants through Centre for Energy Systems Integration (grant number EP/P001173/1), and Thermal Energy Challenge Network (grant number EP/P005667/1), the Newton Fund under the UK-China Joint Research and Innovation Partnership Scheme (Grant No. 201703780098), the National Natural Science Foundation of China (grant numbers 51976176, 51806189), China Science Foundation (grant numbers 2019T120514, 2018M640556), Zhejiang Province Science Foundation (Grant Number ZJ20180099) and Fundamental Research Funds for the Central Universities (grant number

2020QNA4008). The corresponding authors also would like to thank the Cao Guang Biao High Tech Talent Fund from Zhejiang University supporting the collaboration.

References

[1] Roskilly AP, Yan J. Sustainable thermal energy management. Appl Energy 2017;186:249–50.
[2] Dal Magro F, Jimenez-Arreola M, Romagnoli A. Improving energy recovery efficiency by retrofitting a PCM-based technology to an ORC system operating under thermal power fluctuations. Appl Energy 2017;208:972–85.
[3] Jiménez-Arreola M, Pili R, Dal Magro F, Wieland C, Rajoo S, Romagnoli A. Thermal power fluctuations in waste heat to power systems: an overview on the challenges and current solutions. Appl Therm Eng 2018;134:576–84.
[4] Tao YB, He Y-L. A review of phase change material and performance enhancement method for latent heat storage system. Renew Sustain Energy Rev 2018;93:245–59.
[5] Alva G, Lin Y, Fang G. An overview of thermal energy storage systems. Energy 2018;144:341–78.
[6] Raam Dheep G, Sreekumar A. Influence of nanomaterials on properties of latent heat solar thermal energy storage materials – a review. Energy Convers Manage 2014;83:133–48.
[7] Li G, Zheng X. Thermal energy storage system integration forms for a sustainable future. Renew Sustain Energy Rev 2016;62:736–57.
[8] Kenisarin MM. High-temperature phase change materials for thermal energy storage. Renew Sustain Energy Rev 2010;14:955–70.
[9] Gil A, Medrano M, Martorell I, Lázaro A, Dolado P, Zalba B, et al. State of the art on high temperature thermal energy storage for power generation. Part 1—Concepts, materials and modellization. Renew Sustain Energy Rev 2010;14:31–55.
[10] Medrano M, Gil A, Martorell I, Potau X, Cabeza LF. State of the art on high-temperature thermal energy storage for power generation. Part 2—Case studies. Renew Sustain Energy Rev 2010;14:56–72.
[11] Cárdenas B, León N. High temperature latent heat thermal energy storage: Phase change materials, design considerations and performance enhancement techniques. Renew Sustain Energy Rev 2013;27:724–37.
[12] Xu B, Li P, Chan C. Application of phase change materials for thermal energy storage in concentrated solar thermal power plants: A review to recent developments. Appl Energy 2015;160:286–307.
[13] Miró L, Gasia J, Cabeza LF. Thermal energy storage (TES) for industrial waste heat (IWH) recovery: A review. Appl Energy 2016;179:284–301.
[14] Ibrahim NI, Al-Sulaiman FA, Rahman S, Yilbas BS, Sahin AZ. Heat transfer enhancement of phase change materials for thermal energy storage applications: A critical review. Renew Sustain Energy Rev 2017;74:26–50.
[15] Li Q, Li C, Du Z, Jiang F, Ding Y. A review of performance investigation and enhancement of shell and tube thermal energy storage device containing molten salt based phase change materials for medium and high temperature applications. Appl Energy 2019;255:113806.
[16] Manfrida G, Secchi R, Stańczyk K. Modelling and simulation of phase change material latent heat storages applied to a solar-powered Organic Rankine Cycle. Appl Energy 2016;179:378–88.
[17] Jankowski NR, McCluskey FP. A review of phase change materials for vehicle component thermal buffering. Appl Energy 2014;113:1525–61.
[18] Khan MMA, Saidur R, Al-Sulaiman FA. A review for phase change materials (PCMs) in solar absorption refrigeration systems. Renew Sustain Energy Rev 2017;76:105–37.
[19] Zalba B, Marín JM, Cabeza LF, Mehling H. Review on thermal energy storage with phase change: materials, heat transfer analysis and applications. Appl Therm Eng 2003;23:251–83.
[20] Pielichowska K, Pielichowski K. Phase change materials for thermal energy storage. Prog Mater Sci 2014;65:67–123.
[21] Gasia J, Miró L, Cabeza LF. Materials and system requirements of high temperature thermal energy storage systems: A review. Part 2: Thermal conductivity enhancement techniques. Renew Sustain Energy Rev 2016;60:1584–601.
[22] Tay NHS, Liu M, Belusko M, Bruno F. Review on transportable phase change material in thermal energy storage systems. Renew Sustain Energy Rev 2017;75:264–77.
[23] Jaguemont J, Omar N, Van den Bossche P, Mierlo J. Phase-change materials (PCM) for automotive applications: A review. Appl Therm Eng 2018;132:308–20.
[24] Nazir H, Batool M, Bolivar Osorio FJ, Isaza-Ruiz M, Xu X, Vignarooban K, et al. Recent developments in phase change materials for energy storage applications: A review. Int J Heat Mass Transf 2019;129:491–523.
[25] Lin Y, Jia Y, Alva G, Fang G. Review on thermal conductivity enhancement, thermal properties and applications of phase change materials in thermal energy storage. Renew Sustain Energy Rev 2018;82:2730–42.
[26] Alva G, Liu L, Huang X, Fang G. Thermal energy storage materials and systems for solar energy applications. Renew Sustain Energy Rev 2017;68:693–706.
[27] Agyenim F, Hewitt N, Eames P, Smyth M. A review of materials, heat transfer and phase change problem formulation for latent heat thermal energy storage systems (LHTESS). Renew Sustain Energy Rev 2010;14:615–28.
[28] Pereira da Cunha J, Eames P. Thermal energy storage for low and medium temperature applications using phase change materials – A review. Appl Energy 2016;177:227–38.
[29] Al-Abidi AA, Bin Mat S, Sopian K, Sulaiman MY, Lim CH, Th A. Review of thermal energy storage for air conditioning systems. Renew Sustain Energy Rev 2012;16:5802–19.
[30] Haillot D, Bauer T, Kröner U, Tamme R. Thermal analysis of phase change materials in the temperature range 120–150°C. Thermochim Acta 2011;513:49–59.
[31] Wei G, Wang G, Xu C, Ju X, Xing L, Du X, et al. Selection principles and thermophysical properties of high temperature phase change materials for thermal energy storage: A review. Renew Sustain Energy Rev 2018;81:1771–86.
[32] Farkas D, Birchenall CE. New eutectic alloys and their heats of transformation. Metall Trans A 1985;16:323–8.
[33] Mohamed SA, Al-Sulaiman FA, Ibrahim NI, Zahir MH, Al-Ahmed A, Saidur R, et al. A review on current status and challenges of inorganic phase change materials for thermal energy storage systems. Renew Sustain Energy Rev 2017;70:1072–89.
[34] Abdulla MG, Bariyat Yu G. Heat-accumulating properties of melts. Russ Chem Rev 2000;69:179.
[35] Zhang N, Yuan Y, Cao X, Du Y, Zhang Z, Gui Y. Latent heat thermal energy storage systems with solid-liquid phase change materials: a review. Adv Eng Mater 2018;20:1700753.
[36] Raud R, Jacob R, Bruno F, Will G, Steinberg TA. A critical review of eutectic salt property prediction for latent heat energy storage systems. Renew Sustain Energy Rev 2017;70:936–44.
[37] Wang E, Markides CN, Lu Y, Lemort V. Editorial: Organic Rankine cycle for efficiency improvement of industrial processes and urban systems. Front Energy Res 2020;8.
[38] Gomez JC, Calvet N, Starace AK, Glatzmaier GC. Ca(NO3)2—NaNO3—KNO3 molten salt mixtures for direct thermal energy storage systems in parabolic trough plants. J Sol Energy Eng 2013;135:021016–21018.
[39] Cordaro JG, Rubin NC, Bradshaw RW. Multicomponent Molten salt mixtures based on nitrate/nitrite anions. J Sol Energy Eng 2011;133:011014–11024.
[40] Zhang H, Baeyens J, Cáceres G, Degrève J, Lv Y. Thermal energy storage: Recent developments and practical aspects. Prog Energy Combust Sci 2016;53:1–40.
[41] Cabeza LF, Gutierrez A, Barreneche C, Ushak S, Fernández ÁG, Inés Fernádez A, et al. Lithium in thermal energy storage: A state-of-the-art review. Renew Sustain Energy Rev 2015;42:1106–12.
[42] Andraka CE, Kruizenga AM, Hernandez-Sanchez BA, Coker EN. Metallic phase change material thermal storage for dish stirling. Energy Proc 2015;69:726–36.
[43] Sharma A, Tyagi VV, Chen CR, Buddhi D. Review on thermal energy storage with phase change materials and applications. Renew Sustain Energy Rev 2009;13:318–45.
[44] Kenisarin M, Mahkamov K. Solar energy storage using phase change materials. Renew Sustain Energy Rev 2007;11:1913–65.
[45] Birchenall CE, Riechman AF. Heat storage in eutectic alloys. Metall Trans A 1980;11:1415–20.
[46] Rathod MK, Banerjee J. Thermal stability of phase change materials used in latent heat energy storage systems: A review. Renew Sustain Energy Rev 2013;18:246–58.
[47] He Q, Zhang W. A study on latent heat storage exchangers with the high-temperature phase-change material. Int J Energy Res 2001;25:331–41.
[48] Wang X, Liu J, Zhang Y, Di H, Jiang Y. Experimental research on a kind of novel high temperature phase change storage heater. Energy Convers Manage 2006;47:2211–22.
[49] Sun JQ, Zhang RY, Liu ZP, Lu GH. Thermal reliability test of Al–34%Mg–6%Zn alloy as latent heat storage material and corrosion of metal with respect to thermal cycling. Energy Convers Manage 2007;48:619–24.
[50] Khare S, Dell'Amico M, Knight C, McGarry S. Selection of materials for high temperature latent heat energy storage. Sol Energy Mater Sol Cells 2012;107:20–7.
[51] Risueño E, Doppiu S, Rodríguez-Aseguinolaza J, Blanco P, Gil A, Tello M, et al. Experimental investigation of Mg-Zn-Al metal alloys for latent heat storage application. J Alloy Compd 2016;685:724–32.
[52] Fernández AI, Barreneche C, Belusko M, Segarra M, Bruno F, Cabeza LF. Considerations for the use of metal alloys as phase change materials for high temperature applications. Sol Energy Mater Sol Cells 2017;171:275–81.
[53] Crespo A, Barreneche C, Ibarra M, Platzer W. Latent thermal energy storage for solar process heat applications at medium-high temperatures – A review. Sol Energy 2018.
[54] Ma Z, Lin W, Sohel MI. Nano-enhanced phase change materials for improved building performance. Renew Sustain Energy Rev 2016;58:1256–68.
[55] Amaral C, Vicente R, Marques PAAP, Barros-Timmons A. Phase change materials and carbon nanostructures for thermal energy storage: A literature review. Renew Sustain Energy Rev 2017;79:1212–28.
[56] Zhou D, Zhao CY. Experimental investigations on heat transfer in phase change materials (PCMs) embedded in porous materials. Appl Therm Eng 2011;31:970–7.
[57] Pincemin S, Py X, Olives R, Christ M, Oettinger O. Elaboration of conductive thermal storage composites made of phase change materials and graphite for solar plant. J Sol Energy Eng 2007;130:011005–11015.
[58] Zhang P, Xiao X, Meng ZN, Li M. Heat transfer characteristics of a molten-salt thermal energy storage unit with and without heat transfer enhancement. Appl Energy 2015;137:758–72.
[59] Zhu F, Zhang C, Gong X. Numerical analysis on the energy storage efficiency of phase change material embedded in finned metal foam with graded porosity. Appl Therm Eng 2017;123:256–65.
[60] Xu T, Chen Q, Huang G, Zhang Z, Gao X, Lu S. Preparation and thermal energy storage properties of d-Mannitol/expanded graphite composite phase change material. Sol Energy Mater Sol Cells 2016;155:141–6.

[61] Zhao W, France DM, Yu W, Kim T, Singh D. Phase change material with graphite foam for applications in high-temperature latent heat storage systems of concentrated solar power plants. Renew Energy 2014;69:134–46.
[62] Huang Z, Gao X, Xu T, Fang Y, Zhang Z. Thermal property measurement and heat storage analysis of LiNO3/KCl – expanded graphite composite phase change material. Appl Energy 2014;115:265–71.
[63] Zhao YJ, Wang RZ, Wang LW, Yu N. Development of highly conductive KNO3/NaNO3 composite for TES (thermal energy storage). Energy 2014;70:272–7.
[64] Xiao X, Zhang P, Li M. Experimental and numerical study of heat transfer performance of nitrate/expanded graphite composite PCM for solar energy storage. Energy Convers Manage 2015;105:272–84.
[65] Singh D, Zhao W, Yu W, France DM, Kim T. Analysis of a graphite foam–NaCl latent heat storage system for supercritical CO2 power cycles for concentrated solar power. Sol Energy 2015;118:232–42.
[66] Singh D, Kim T, Zhao W, Yu W, France DM. Development of graphite foam infiltrated with MgCl2 for a latent heat based thermal energy storage (LHTES) system. Renew Energy 2016;94:660–7.
[67] Wu ZG, Zhao CY. Experimental investigations of porous materials in high temperature thermal energy storage systems. Sol Energy 2011;85:1371–80.
[68] Zhao CY, Wu ZG. Heat transfer enhancement of high temperature thermal energy storage using metal foams and expanded graphite. Sol Energy Mater Sol Cells 2011;95:636–43.
[69] Li Z, Wu Z-G. Numerical study on the thermal behavior of phase change materials (PCMs) embedded in porous metal matrix. Sol Energy 2014;99:172–84.
[70] Zhong L, Zhang X, Luan Y, Wang G, Feng Y, Feng D. Preparation and thermal properties of porous heterogeneous composite phase change materials based on molten salts/expanded graphite. Sol Energy 2014;107:63–73.
[71] Tao YB, Lin CH, He YL. Preparation and thermal properties characterization of carbonate salt/carbon nanomaterial composite phase change material. Energy Convers Manage 2015;97:103–10.
[72] Chaxiu G, Yahui W. Numerical investigation of nanoparticle-enhanced high temperature phase change material for solar energy storage. Adv Mater Res 2012;512–515:961–4.
[73] Myers PD, Alam TE, Kamal R, Goswami DY, Stefanakos E. Nitrate salts doped with CuO nanoparticles for thermal energy storage with improved heat transfer. Appl Energy 2016;165:225–33.
[74] Babapoor A, Karimi G. Thermal properties measurement and heat storage analysis of paraffinnanoparticles composites phase change material: Comparison and optimization. Appl Therm Eng 2015;90:945–51.
[75] Dsilva Winfred Rufuss D, Suganthi L, Iniyan S, Davies PA. Effects of nanoparticle-enhanced phase change material (NPCM) on solar still productivity. J Cleaner Prod 2018;192:9–29.
[76] He Q, Wang S, Tong M, Liu Y. Experimental study on thermophysical properties of nanofluids as phase-change material (PCM) in low temperature cool storage. Energy Convers Manage 2012;64:199–205.
[77] Zhang Z, Yuan Y, Alelyani S, Cao X, Phelan PE. Thermophysical properties enhancement of ternary carbonates with carbon materials for high-temperature thermal energy storage. Sol Energy 2017;155:661–9.
[78] Han D, Guene Lougou B, Xu Y, Shuai Y, Huang X. Thermal properties characterization of chloride salts/nanoparticles composite phase change material for high-temperature thermal energy storage. Appl Energy 2020;264:114674.
[79] Nomura T, Tabuchi K, Zhu C, Sheng N, Wang S, Akiyama T. High thermal conductivity phase change composite with percolating carbon fiber network. Appl Energy 2015;154:678–85.
[80] Jurčević M, Nižetić S, Arıcı M, Ocłoń P. Comprehensive analysis of preparation strategies for phase change nanocomposites and nanofluids with brief overview of safety equipment. J Cleaner Prod 2020;274:122963.
[81] Tao YB, Lin CH, He YL. Effect of surface active agent on thermal properties of carbonate salt/carbon nanomaterial composite phase change material. Appl Energy 2015;156:478–89.
[82] Ye F, Ge Z, Ding Y, Yang J. Multi-walled carbon nanotubes added to Na2CO3/MgO composites for thermal energy storage. Particuology 2014;15:56–60.
[83] Yang C, Navarro ME, Zhao B, Leng G, Xu G, Wang L, et al. Thermal conductivity enhancement of recycled high density polyethylene as a storage media for latent heat thermal energy storage. Sol Energy Mater Sol Cells 2016;152:103–10.
[84] Pincemin S, Olives R, Py X, Christ M. Highly conductive composites made of phase change materials and graphite for thermal storage. Sol Energy Mater Sol Cells 2008;92:603–13.
[85] Seki Y, İnce Ş, Ezan MA, Turgut A, Erek A. Graphite nanoplates loading into eutectic mixture of Adipic acid and Sebacic acid as phase change material. Sol Energy Mater Sol Cells 2015;140:457–63.
[86] Zhang Q, Luo Z, Guo Q, Wu G. Preparation and thermal properties of short carbon fibers/erythritol phase change materials. Energy Convers Manage 2017;136:220–8.
[87] Seeniraj RV, Lakshmi Narasimhan N. Performance enhancement of a solar dynamic LHTS module having both fins and multiple PCMs. Sol Energy 2008;82:535–42.
[88] Agyenim F, Eames P, Smyth M. A comparison of heat transfer enhancement in a medium temperature thermal energy storage heat exchanger using fins. Sol Energy 2009;83:1509–20.
[89] Steinmann W-D, Laing D, Tamme R. Development of PCM storage for process heat and power generation. J Sol Energy Eng 2009;131:041009–41014.
[90] Bayón R, Rojas E, Valenzuela L, Zarza E, León J. Analysis of the experimental behaviour of a 100 kWth latent heat storage system for direct steam generation in solar thermal power plants. Appl Therm Eng 2010;30:2643–51.
[91] Tao YB, He YL, Qu ZG. Numerical study on performance of molten salt phase change thermal energy storage system with enhanced tubes. Sol Energy 2012;86:1155–63.
[92] Parry AJ, Eames PC, Agyenim FB. Modeling of thermal energy storage shell-and-tube heat exchanger. Heat Transfer Eng 2013;35:1–14.
[93] Tiari S, Qiu S, Mahdavi M. Numerical study of finned heat pipe-assisted thermal energy storage system with high temperature phase change material. Energy Convers Manage 2015;89:833–42.
[94] Zauner C, Hengstberger F, Etzel M, Lager D, Hofmann R, Walter H. Experimental characterization and simulation of a fin-tube latent heat storage using high density polyethylene as PCM. Appl Energy 2016;179:237–46.
[95] Wang P, Yao H, Lan Z, Peng Z, Huang Y, Ding Y. Numerical investigation of PCM melting process in sleeve tube with internal fins. Energy Convers Manage 2016;110:428–35.
[96] Sivasamy P, Devaraju A, Harikrishnan S. Review on Heat Transfer Enhancement of Phase Change Materials (PCMs). Mater Today: Proc 2018;5:14423–31.
[97] Tao YB, He YL. Effects of natural convection on latent heat storage performance of salt in a horizontal concentric tube. Appl Energy 2015;143:38–46.
[98] Elmaazouzi Z, El Alami M, Gounni A, Bennouna EG. Thermal energy storage with phase change materials: Application on coaxial heat exchanger with fins. Mater Today: Proc 2020;27:3095–100.
[99] Elmaazouzi Z, El Alami M, Agalit H, Bennouna EG. Performance evaluation of latent heat TES system-case study: Dimensions improvements of annular fins exchanger. Energy Rep 2020;6:294–301.
[100] Yıldız Ç, Arıcı M, Nižetić S, Shahsavar A. Numerical investigation of natural convection behavior of molten PCM in an enclosure having rectangular and tree-like branching fins. Energy 2020;207:118223.
[101] Ji C, Qin Z, Dubey S, Choo FH, Duan F. Simulation on PCM melting enhancement with double-fin length arrangements in a rectangular enclosure induced by natural convection. Int J Heat Mass Transf 2018;127:255–65.
[102] Jmal I, Baccar M. Numerical investigation of PCM solidification in a finned rectangular heat exchanger including natural convection. Int J Heat Mass Transf 2018;127:714–27.
[103] Brahim T, Dhaou MH, Jemni A. Theoretical and experimental investigation of plate screen mesh heat pipe solar collector. Energy Convers Manage 2014;87:428–38.
[104] Shabgard H, Bergman TL, Sharifi N, Faghri A. High temperature latent heat thermal energy storage using heat pipes. Int J Heat Mass Transf 2010;53:2979–88.
[105] Nithyanandam K, Pitchumani R. Computational studies on a latent thermal energy storage system with integral heat pipes for concentrating solar power. Appl Energy 2013;103:400–15.
[106] Nithyanandam K, Pitchumani R. Analysis and optimization of a latent thermal energy storage system with embedded heat pipes. Int J Heat Mass Transf 2011;54:4596–610.
[107] Nithyanandam K, Pitchumani R. Design of a latent thermal energy storage system with embedded heat pipes. Appl Energy 2014;126:266–80.
[108] Shabgard H, Robak CW, Bergman TL, Faghri A. Heat transfer and exergy analysis of cascaded latent heat storage with gravity-assisted heat pipes for concentrating solar power applications. Sol Energy 2012;86:816–30.
[109] Sharifi N, Faghri A, Bergman TL, Andraka CE. Simulation of heat pipe-assisted latent heat thermal energy storage with simultaneous charging and discharging. Int J Heat Mass Transf 2015;80:170–9.
[110] Liu Z, Wang Z, Ma C. An experimental study on heat transfer characteristics of heat pipe heat exchanger with latent heat storage. Part I: Charging only and discharging only modes. Energy Convers Manage 2006;47:944–66.
[111] Liu Z, Wang Z, Ma C. An experimental study on the heat transfer characteristics of a heat pipe heat exchanger with latent heat storage. Part II: Simultaneous charging/discharging modes. Energy Convers Manage 2006;47:967–91.
[112] Tiari S, Qiu S. Three-dimensional simulation of high temperature latent heat thermal energy storage system assisted by finned heat pipes. Energy Convers Manage 2015;105:260–71.
[113] Tiari S, Qiu S, Mahdavi M. Discharging process of a finned heat pipe–assisted thermal energy storage system with high temperature phase change material. Energy Convers Manage 2016;118:426–37.
[114] Hu B-w, Wang Q, Liu Z-H. Fundamental research on the gravity assisted heat pipe thermal storage unit (GAHP-TSU) with porous phase change materials (PCMs) for medium temperature applications. Energy Convers Manage 2015;89:376–86.
[115] Liu Z-h, Zheng B-c, Wang Q, Li S-S. Study on the thermal storage performance of a gravity-assisted heat-pipe thermal storage unit with granular high-temperature phase-change materials. Energy 2015;81:754–65.
[116] Song H-j, Zhang W, Li Y-q, Yang Z-W, Ming A-B. Exergy analysis and parameter optimization of heat pipe receiver with integrated latent heat thermal energy storage for space station in charging process. Appl Therm Eng 2017;119:304–11.
[117] Elsanusi OS, Nsofor EC. Melting of multiple PCMs with different arrangements inside a heat exchanger for energy storage. Appl Therm Eng 2020;116046.
[118] Zhen X, Mujumdar AS. Cyclic heat transfer in a novel storage unit of multiple phase change materials. Appl Therm Eng 1996;16:807–15.
[119] Gong Z-X, Mujumdar AS. Thermodynamic optimization of the thermal process in energy storage using multiple phase change materials. Appl Therm Eng 1997;17:1067–83.
[120] Li YQ, He YL, Song HJ, Xu C, Wang WW. Numerical analysis and parameters optimization of shell-and-tube heat storage unit using three phase change materials. Renew Energy 2013;59:92–9.

[121] Wang P, Wang X, Huang Y, Li C, Peng Z, Ding Y. Thermal energy charging behaviour of a heat exchange device with a zigzag plate configuration containing multi-phase-change-materials (m-PCMs). Appl Energy 2015;142:328–36.
[122] Yuan F, Li M-J, Ma Z, Jin B, Liu Z. Experimental study on thermal performance of high-temperature molten salt cascaded latent heat thermal energy storage system. Int J Heat Mass Transf 2018;118:997–1011.
[123] Cui H, Yuan X, Hou X. Thermal performance analysis for a heat receiver using multiple phase change materials. Appl Therm Eng 2003;23:2353–61.
[124] Michels H, Pitz-Paal R. Cascaded latent heat storage for parabolic trough solar power plants. Sol Energy 2007;81:829–37.
[125] Mostafavi Tehrani SS, Shoraka Y, Nithyanandam K, Taylor RA. Cyclic performance of cascaded and multi-layered solid-PCM shell-and-tube thermal energy storage systems: A case study of the 19.9 MW e Gemasolar CSP plant. Appl Energy 2018;228:240–53.
[126] Peiró G, Gasia J, Miró L, Cabeza LF. Experimental evaluation at pilot plant scale of multiple PCMs (cascaded) vs. single PCM configuration for thermal energy storage. Renew Energy 2015;83:729–36.
[127] Tao YB, He YL. Numerical study on performance enhancement of shell-and-tube latent heat storage unit. Int Commun Heat Mass Transfer 2015;67:147–52.
[128] Elfeky KE, Ahmed N, Wang Q. Numerical comparison between single PCM and multi-stage PCM based high temperature thermal energy storage for CSP tower plants. Appl Therm Eng 2018;139:609–22.
[129] Shamsi H, Boroushaki M, Geraei H. Performance evaluation and optimization of encapsulated cascade PCM thermal storage. J Storage Mater 2017;11:64–75.
[130] Wu M, Xu C, He Y. Cyclic behaviors of the molten-salt packed-bed thermal storage system filled with cascaded phase change material capsules. Appl Therm Eng 2016;93:1061–73.
[131] Legmann H. Recovery of industrial heat in the cement industry by means of the ORC process. IEEE-IAS/PCS 2002 cement industry technical conference record (Cat No02CH37282); 2002. p. 29–35.
[132] Brandt C, Schüler N, Gaderer M, Kuckelkorn JM. Development of a thermal oil operated waste heat exchanger within the off-gas of an electric arc furnace at steel mills. Appl Therm Eng 2014;66:335–45.
[133] Petr P, Tegethoff W, Köhler J. Method for designing waste heat recovery systems (WHRS) in vehicles considering optimal control. Energy Proc 2017;129:232–9.
[134] Guo C, Zhang W. Numerical simulation and parametric study on new type of high temperature latent heat thermal energy storage system. Energy Convers Manage 2008;49:919–27.
[135] Robak CW, Bergman TL, Faghri A. Economic evaluation of latent heat thermal energy storage using embedded thermosyphons for concentrating solar power applications. Sol Energy 2011;85:2461–73.
[136] Mahfuz MH, Kamyar A, Afshar O, Sarraf M, Anisur MR, Kibria MA, et al. Exergetic analysis of a solar thermal power system with PCM storage. Energy Convers Manage 2014;78:486–92.
[137] Casati E, Galli A, Colonna P. Thermal energy storage for solar-powered organic Rankine cycle engines. Sol Energy 2013;96:205–19.
[138] Freeman J, Guarracino I, Kalogirou SA, Markides CN. A small-scale solar organic Rankine cycle combined heat and power system with integrated thermal energy storage. Appl Therm Eng 2017;127:1543–54.
[139] Li S, Ma H, Li W. Dynamic performance analysis of solar organic Rankine cycle with thermal energy storage. Appl Therm Eng 2018;129:155–64.
[140] D. L, T. B, W. D, Steinmann DL. Advanced high temperature latent heat storage system – design and test results. Stockholm, Sweden; 2009. p. 8.
[141] Laing D, Bahl C, Bauer T, Lehmann D, Steinmann W-D. Thermal energy storage for direct steam generation. Sol Energy 2011;85:627–33.
[142] Adinberg R, Zvegilsky D, Epstein M. Heat transfer efficient thermal energy storage for steam generation. Energy Convers Manage 2010;51:9–15.
[143] Miró L, Brückner S, Cabeza LF. Mapping and discussing Industrial Waste Heat (IWH) potentials for different countries. Renew Sustain Energy Rev 2015;51:847–55.
[144] Brückner S, Liu S, Miró L, Radspieler M, Cabeza LF, Lävemann E. Industrial waste heat recovery technologies: An economic analysis of heat transformation technologies. Appl Energy 2015;151:157–67.
[145] Maruoka N, Sato K, Yagi J-i, Akiyama T. Development of PCM for recovering high temperature waste heat and utilization for producing hydrogen by reforming reaction of methane. ISIJ Int 2002;42:215–9.
[146] Maruoka N, Akiyama T. Thermal stress analysis of PCM encapsulation for heat recovery of high temperature waste heat. J Chem Eng Jpn 2003;36:794–8.
[147] Maruoka N, Mizuochi T, Purwanto H, Akiyama T. Feasibility study for recovering waste heat in the steelmaking industry using a chemical recuperator. ISIJ Int 2004;44:257–62.
[148] Maruoka N, Akiyama T. Exergy recovery from steelmaking off-gas by latent heat storage for methanol production. Energy 2006;31:1632–42.
[149] R. de B, S.F. S, P.W. B. Heat storage systems for use in an industrial batch process: (results of) a case study. The tenth international conference on thermal energy storage. ECOSTOCK, New Jersey, USA; 2006.
[150] Nardin G, Meneghetti A, Dal Magro F, Benedetti N. PCM-based energy recovery from electric arc furnaces. Appl Energy 2014;136:947–55.
[151] Dal Magro F, Meneghetti A, Nardin G, Savino S. Enhancing energy recovery in the steel industry: Matching continuous charge with off-gas variability smoothing. Energy Convers Manage 2015;104:78–89.
[152] Dal Magro F, Benasciutti D, Nardin G. Thermal stress analysis of PCM containers for temperature smoothing of waste gas. Appl Therm Eng 2016;106:1010–22.
[153] Dal Magro F, Savino S, Meneghetti A, Nardin G. Coupling waste heat extraction by phase change materials with superheated steam generation in the steel industry. Energy 2017;137:1107–18.
[154] Dal Magro F, Xu H, Nardin G, Romagnoli A. Application of high temperature phase change materials for improved efficiency in waste-to-energy plants. Waste Manage 2018;73:322–31.
[155] Takuya N. Non-conduit heat distribution using waste heat from a sewage sludge incinerator; 2007.
[156] Nomura T, Okinaka N, Akiyama T. Waste heat transportation system, using phase change material (PCM) from steelworks to chemical plant. Resour Conserv Recycl 2010;54:1000–6.
[157] Guo S, Li H, Zhao J, Li X, Yan J. Numerical simulation study on optimizing charging process of the direct contact mobilized thermal energy storage. Appl Energy 2013;112:1416–23.
[158] Li H, Wang W, Yan J, Dahlquist E. Economic assessment of the mobilized thermal energy storage (M-TES) system for distributed heat supply. Appl Energy 2013;104:178–86.
[159] Wang W, Guo S, Li H, Yan J, Zhao J, Li X, et al. Experimental study on the direct/indirect contact energy storage container in mobilized thermal energy system (M-TES). Appl Energy 2014;119:181–9.
[160] Guo S, Zhao J, Wang W, Jin G, Wang X, An Q, et al. Experimental study on solving the blocking for the direct contact mobilized thermal energy storage container. Appl Therm Eng 2015;78:556–64.
[161] Chiu JN, Castro Flores J, Martin V, Lacarrière B. Industrial surplus heat transportation for use in district heating. Energy 2016;110:139–47.
[162] Zhang X, Chen X, Han Z, Xu W. Study on phase change interface for erythritol with nano-copper in spherical container during heat transport. Int J Heat Mass Transf 2016;92:490–6.
[163] Guo S, Zhao J, Wang W, Yan J, Jin G, Wang X. Techno-economic assessment of mobilized thermal energy storage for distributed users: A case study in China. Appl Energy 2017;194:481–6.
[164] Guo S, Liu Q, Zhao J, Jin G, Wu W, Yan J, et al. Mobilized thermal energy storage: Materials, containers and economic evaluation. Energy Convers Manage 2018;177:315–29.
[165] Maruoka N, Akiyama T. Development of PCM reactor for methane steam reforming. ISIJ Int 2010;50:1305–10.
[166] Vasiliev LL, Burak VS, Kulakov AG, Mishkinis DA, Bohan PV. Latent heat storage modules for preheating internal combustion engines: application to a bus petrol engine. Appl Therm Eng 2000;20:913–23.
[167] Gumus M. Reducing cold-start emission from internal combustion engines by means of thermal energy storage system. Appl Therm Eng 2009;29:652–60.
[168] Gopal KN, Subbarao R, Pandiyarajan V, Velraj R. Thermodynamic analysis of a diesel engine integrated with a PCM based energy storage system. Int J Thermodyn 2010;13:15–21.
[169] Pandiyarajan V, Chinna Pandian M, Malan E, Velraj R, Seeniraj RV. Experimental investigation on heat recovery from diesel engine exhaust using finned shell and tube heat exchanger and thermal storage system. Appl Energy 2011;88:77–87.
[170] Pandiyarajan V, Chinnappandian M, Raghavan V, Velraj R. Second law analysis of a diesel engine waste heat recovery with a combined sensible and latent heat storage system. Energy Policy 2011;39:6011–20.
[171] Pandiyarajan V, Prabhu A, Velraj R. Experimental investigation of a cascaded latent heat storage system for diesel engine waste heat recovery AU - Chinnapandian, M. Energy Sources Part A: Recovery, Utilizat, Environ Effects 2015;37:1308–17.
[172] Prabu SS, M.A A. A study of waste heat recovery from diesel engine exhaust using phase change material. Int J ChemTech Res 2015;8:7.
[173] Shon J, Kim H, Lee K. Improved heat storage rate for an automobile coolant waste heat recovery system using phase-change material in a fin–tube heat exchanger. Appl Energy 2014;113:680–9.
[174] Yu X, Li Z, Lu Y, Huang R, Roskilly AP. Investigation of organic Rankine cycle integrated with double latent thermal energy storage for engine waste heat recovery. Energy 2019;170:1098–112.
[175] Du K, Calautit J, Wang Z, Wu Y, Liu H. A review of the applications of phase change materials in cooling, heating and power generation in different temperature ranges. Appl Energy 2018;220:242–73.
[176] Gulfam R, Zhang P, Meng Z. Advanced thermal systems driven by paraffin-based phase change materials – A review. Appl Energy 2019;238:582–611.
[177] Chau KT, Chan CC. Emerging energy-efficient technologies for hybrid electric vehicles. Proc IEEE 2007;95:821–35.